Estimation of the area-specific suspended sediment yield from discrete samples in different regions of Belgium

Jean Van Campenhout[1] · François Petit[1] · Alexandre Peeters[1] · Geoffrey Houbrechts[1]

Abstract

Purpose Suspended sediment transport, which represents the majority of the sediment load, has been studied across very different scales and in a wide variety of regions and climates. Despite numerous studies, data for European watersheds are generally limited and correspond to large rivers systems. Especially, in Belgium, little data is available outside the Belgian loess belt. Moreover, the high heterogeneity of soil erosion and sediment transport makes it difficult to measure or model at watershed scale. The purpose of this research is to estimate the median sediment yields in different geographical regions and to detect their explanatory variables.

Materials and methods Gathering data from 1994 to 2016, more than 2000 measurements of suspended sediment concentration at 72 river stations mainly located in South-Belgium were sampled according to a flood-event-based manual methodology. This allowed fast acquisition of data in watersheds ranging from 7 to 3600 km^2 in different geographical regions. Median area-specific sediment yields (SSY) were calculated at watershed scale while looking for regional differences.

Results and discussion Median area-specific sediment yields computed for the period 1996–2018 show regional differences: 19.2 t km^{-2} $year^{-1}$ on sandy substrate (Lorraine), 24.9 t km^{-2} $year^{-1}$ on schisto-sandstone substratum (Ardenne), and up to 119 t km^{-2} $year^{-1}$ in the loamy Brabant plateau, with a link to the agricultural land cover and, to a lesser extent, to the watershed slope. The high temporal and spatial variability of rainfall has great effects on the SSY, necessitating the gathering of more than 20 years of data to smooth the high variability of SSY. A multiple correlation of land cover variables and the average slope of the watershed with SSY managed to explain 48% of the variance within the SSY observations.

Conclusions The agricultural land cover has an important effect on median SSY values. While the regionalization of Belgium is largely based on lithology, soils, and altitude, the land use resulting from these physical and climatic characteristics explains the differences in SSY. Field values of clogged dams and waterways confirm the matching of the SSY computation from discrete samples, despite the high temporal variability of sediment transport.

Keywords Sediment yield · Suspended sediment concentration · Soil erosion rate · Meuse basin · Scheldt basin

1 Introduction

The area-specific sediment yield (SSY), expressed in t km^{-2} $year^{-1}$, is the amount of sediment that is exported out of a given watershed. The SSY of a large diversity of watersheds has been studied worldwide since the nineteenth century and measured with increasing accuracy due to recent technological improvements (Asselman 2000; Verstraeten and Poesen 2001; Ward 2008; Métadier and Bertrand-Krajewski 2012). These studies have been conducted in a wide range of watershed scales, with different lithologies and climates (Moatar et al. 2006; Dumas 2007; Lefrançois et al. 2007; Picouet et al. 2009; Furuichi et al. 2009; Mano et al. 2009; Marttila and Kløve 2010; Oeurng et al. 2010; Gao and Josefson 2012; Araujo et al. 2012; Fortesa et al. 2021). They often showed a link between SSY and land cover, amount, and intensity of rainfall as well as the availability of fine sediment in the watersheds. For instance, the effects on SSY of heavy summer precipitation have been studied on the Mediterranean rim (Seeger

et al. 2004; Nadal-Romero et al. 2008; Tena et al. 2011), the temporal distribution of soil erosion examined in high relief energy areas (Jansson 1996; Sadeghi et al. 2008; Navratil et al. 2011), and the variability of sediment transport analysed at spatial scale (Steegen et al. 1998; Lenzi and Marchi 2000; Meybeck et al. 2003; Vanmaercke et al. 2012b; Gericke and Venohr 2012). Impacts of traditional soil conservation practices were observed (Estrany et al. 2009), in terms of reducing soil erosion by an order of magnitude. Also widely analysed were the effect of wildfires on the increase of soil erosion (Lane et al. 2006; Warrick et al. 2015). Many sedimentary studies also showed the ecological impacts of sediment accumulation on stream habitats (Parkinson et al. 1999; Tramblay et al. 2010; Collins et al. 2011); some authors associated it to a decrease of biodiversity in silt-clogged river beds (Vaessen et al. 2021), while others to human impacts on sediment yield resulting in the consolidation of riverbanks or an increase of flooding risks (Dumas 2007; Vanmaercke et al. 2015).

In Europe, the analysis performed by Vanmaercke et al. (2011, 2012a) combining data from 1794 watersheds in Europe (area: 0.01–1,360,000 km^2) showed that the average erosion rate observed in Europe was 341 t km^{-2} $year^{-1}$, for a median rate of 92 t km^{-2} $year^{-1}$, with six orders of magnitude separating the minimum values (0.3 t km^{-2} $year^{-1}$) from the maximum values (30,000 t km^{-2} $year^{-1}$). These differences were attributed to a combination of factors, such as differences in climate, topography, lithology, and land use (Vanmaercke et al. 2011).

This present study is intended to compensate for the lack of published quantified data on suspended sediment transport in rivers of the southern part of Belgium (Wallonia). Because of the influx of fine sediments into the waterways surrounding loamy soils, public river managers needed to know, for a large number of stations, the quantity of transported sediments, and their geographical origin, identified using reference stations in other regions with different lithology, land cover, and physical characteristics.

Indeed, suspended sediment concentrations (SSC) and SSY estimations have mainly been carried out, in Belgium, on watersheds of medium size, from agronomic researches at plot scale, up to watershed synthetic analyses (Steegen et al. 1998; Verstraeten and Poesen 2001; Pineux 2018). Vanmaercke et al. (2011) have highlighted the lack of sediment transport studies over long periods in large watersheds in Belgium (often < 100 km^2 and mainly located in the Scheldt basin in loamy environment). For instance, the Dyle watershed showed SSY of 30 t km^{-2} $year^{-1}$ in 1959–1960 at Leuven (742 km^2), 70 t km^{-2} $year^{-1}$ in 1985–1986 at Bertem (730 km^2), and 210 t km^{-2} $year^{-1}$ in 1998–2000 downstream of Leuven (820 km^2) (Boardman and Poesen 2006). Other measurement campaigns were also carried out since the end of the nineteenth century in the Meuse and Scheldt watersheds (Spring and Prost 1884; Close-Lecocq et al. 1982; Lemin 1984; Lemin et al. 1987; Ward 2008) or some of their tributaries (Sine and Agneessens 1978; Petit 1985; Lemin et al. 1987; Lamalle et al. 1989; Perpinien 1998; Parkinson et al. 1999; Hombrouckx 2002; Monseur 2005). However, changes in land cover and agricultural practices are known to have great effect upon soil erosion, and therefore, updated SSY values encompassing rivers in different geographical regions were of interest for managers. A fairly rapid and inexpensive methodology was developed during two successive research projects (between 2006 and 2011) on watersheds ranging in size from 7 to 3600 km^2 to estimate SSY in rivers located in the southern part of Belgium.

2 Materials and methods

2.1 Study location: geographical and geological features

The 72 study sites correspond to gauging stations which are located in Wallonia, the southern region of Belgium. A total of 65 of them belong to the Meuse basin, 6 to the Scheldt basin, and 1 to the Moselle basin (see Table 1; Fig. 1). This area experiences a warm-temperate and oceanic climate without a dry season (*Cfb* code in the updated Köppen-Geiger classification) and encounters annual rainfall ranging from 725 mm in westernmost Wallonia to 1400 mm in the easternmost part of the region, mainly in relation to the elevation gradient (Erpicum et al. 2018). The selection of sites where SSY have been quantified through SSC measurements has been guided by the presence of flow gauging stations. After preliminary results were acquired on major rivers, the sampling network has been extended to watersheds of lesser area and/or in other geographical regions while the set of installed gauging stations was growing in Wallonia under the aegis of the public service. The 72 stations are distributed as shown in Fig. 1 in the different geographical regions. The regional classification of stations depends on their location and on the sedimentary setting and the hydrological dynamics of the upstream area. The regional affiliation of each station (Van Campenhout et al. 2020) is shown in Table 2 as well as their geological substratum and loess availability. The land cover proportion in each watershed is derived from Copernicus Land Service and the Corine Land Cover maps (Panagos et al. 2015; CORINE Land Cover 2018). These 100-m resolution maps have been reclassified to give the spatial proportion of forest, grassland, cultivated area, and impervious area at watershed scale with the raw data available for the years 2000, 2006, 2012, and 2018 (Table 9 in Supplementary Material).

Table 1 Characteristics of the studied watersheds

#	River	Location	Basin area (km^2)	$Q_{b \text{ (hourly data)}}$ (m^3 s^{-1})	Source of $Q_{b \text{ (hourly data)}}$ values
ARDENNE					
1	Aisne	Erezée (L6690)	67.4	7.3	Houbrechts (2000)
2	Aisne	Juzaine (L5491)	183	23.8	Houbrechts (2000)
3	Amblève	Targnon (S6671)	802.9	87.3	New obs.
4	Amblève	Martinrive Nonceveux (S6621)	1,064.5 992.8	140	Houbrechts (2005)
5	Chavanne	Vaux-Chavanne (ULiege data)	12	2.9	Houbrechts et al. (2015)
6	Eau Noire	Couvin (L6350)	102	32.1	Computed $Q_{0.625}$
7	Hédrée	Hargimont (L6940)	45.1	13.8	Computed $Q_{0.625}$
8	Hoëgne	Belleheid (S6526)	20	10	New obs. (2019)
9	Hoëgne	Theux (L5860)	189	36.8	Deroanne (1995)
10	Lembrée	Vieuxville (L6300)	51	7.9	Houbrechts (2005)
11	Lesse	Lessive (L6360 + L5080) Villers-sur-Lesse	897 1,090	64.3 99.5	Computed $Q_{0.625}$ Peeters et al. (2018)
12	Lesse	Hérock (L6610)	1,156	105	Bioengineering techniques report (2016)
13	Lhomme	Grupont (L6360)	179.9	20	Franchimont (1993)
14	Lhomme	Rochefort (L6650)	424.9	51.8	Computed $Q_{0.625}$
15	Lhomme	Eprave (L6360)	478	60	Petit et al. (2015)
16	Lienne	Lorcé (L6240)	147	21.3	Houbrechts 2005 and new obs. (2008)
17	Mellier	Marbehan (L5500)	62	8.8	New obs. (2008)
18	Ourthe occidentale	Amberloup (L6290)	109	13	New obs. (2020)
19	Ourthe orientale	Houffalize (L5930)	179	21	Petit et al. 2015
20	Ourthe	Méry Sauheid (S5857)	2,691 2,910	295 300	$Q_b = 0.1346\,A^{0.974}$ (Petit et al. 2007) Pauquet and Petit (1993)
21	Ourthe	Liège (Angleur) $Q_{\text{Sauheid}} + Q_{\text{Chaudfontaine}}$	3,624	394	$Q_b = 0.1346\,A^{0.974}$ (Petit et al. 2007)
22	Rulles	Forêt d'Anlier	16	1.3	Petit (1987)
23	Rulles	Habay-la-Vieille (L5970)	96	11	Petit and Pauquet (1997)
24	Rulles	Tintigny (L5220)	219	24.3	New. obs. (2008)
25	Salm	Trois-Ponts (L6070)	202	24	Louette (1995)
26	Semois	Tintigny (S9561)	380.9	40	Auth. obs. (2008)
27	Sûre	Martelange (L5610)	209	32	Peeters et al. (2018)
28	Vesdre	Chaudfontaine (S6228)	683	120	Petit and Daxhelet (1989)
29	Vierre	Suxy (L7140)	219.8	19	New obs. (2008)
30	Viroin	Olloy-sur-Viroin (L6380)	491	55	New obs. (2011)
31	Viroin	Treignes (L6760)	542.4	62	New obs. (2009)
32	Wamme	Hargimont (old station L6370)	80	12.1	New obs. (2008)
33	Wayai	Spixhe (L6790)	93.8	25	New estimate
HAINE BASIN					
34	Anneau	Marchipont (L6870)	78.2	7.3	Computed $Q_{0.625}$
35	Grande Honnelle	Baisieux (L5170)	121	12.4	Computed $Q_{0.625}$
36	R$^{\text{au}}$ des Estinnes	Estinnes-au-Val (L7080)	28.7	3.0	Computed $Q_{0.625}$
37	Trouille	Givry (L6710)	55.7	4.2	Computed $Q_{0.625}$
38	Trouille	Harmignies (L6430)	79.9	4.1	Computed $Q_{0.625}$
39	Trouille	Spiennes (L6600)	93	3.6	Computed $Q_{0.625}$
40	Trouille	Hyon (S3643)	224	8.9	Computed $Q_{0.625}$
CONDROZ					
41	Bocq	Spontin (L7320)	163.6	18.3	Petit et al. (2015)
42	Bocq	Yvoir (L5800)	230	26.3	Peeters et al. (2020)

Table 1 (continued)

#	River	Location	Basin area (km²)	$Q_{b \text{ (hourly data)}}$ (m³ s⁻¹)	Source of $Q_{b \text{ (hourly data)}}$ values
43	Somme	Petite-Somme (ULiege data)	37.3	4	Houbrechts (2005) and new obs. (2007)
ENTRE-VESDRE-ET-MEUSE					
44	Berwinne	Dalhem (L6390)	118	17	Houbrechts et al. (2015)
45	Bolland	Dalhem (L6770)	29.3	3.4	New obs.
46	Gueule	Sippenaeken (L6660)	121	16	Mols (2004)
47	Magne	Prayon/Foret (L6780/L7600)	40.5	4.7	Computed $Q_{0.625}$
FAGNE-FAMENNE					
48	Biran	Wanlin (L7190)	51.9	6.3	New obs. (2008)
49	Brouffe	Mariembourg (S9111)	80	20	New obs. (2009)
50	Eau Blanche	Aublain (L6530)	106.2	17	Peeters et al. (2021)
51	Hermeton	Romedenne (L5060)	115	17.3	New obs. (2008)
52	Marchette	Marche-en-Famenne (L7120)	48.9	7.2	Petit and Daxhelet (1989)
53	R^{au} d'Heure	Baillonville (L6050)	68	14	Louette (1995) and new obs. (2020)
54	Wimbe	Lavaux-Sainte-Anne (L6270)	93	15	New obs. (2020)
HESBAYE					
55	Burdinale	Lamontzée	7.2	0.8	Lamalle et al. (1989)
56	Burdinale	Marneffe (L6461)	26.8	2.2	Computed $Q_{0.625}$
57	Geer	Eben-Emael (L6340)	452.3	11.9	Mabille and Petit (1987)(1987
58	Mehaigne	Wanze (L5820)	352.1	11.2	Computed $Q_{0.625}$
		Moha	345	18.1	(Perpinien 1998)
59	Petite Gette	Opheylissem (L6280)	134	4.8	Computed $Q_{0.625}$
60	Petite Gette	Zoutleeuw (L09_154)	276	5.3 (6.3)	Computed $Q_{0.625}$ (Hombrouckx 2002)
61	Grande Gette	Sainte-Marie-Geest (L5720)	135	8.7 (10)	Computed $Q_{0.625}$ (New est., 2011)
62	Gette	Halen (L09_152)	805	17.7 (21)	Computed $Q_{0.625}$ (Hombrouckx 2002)
LORRAINE					
63	Chavratte	Dampicourt (L7060)	55.9	2.4	Computed $Q_{0.625}$
64	Semois	Chantemelle (L5880)	89	11.1	New obs. (2001); Hallot (2010)
65	Semois	Etalle (L6180)	123.9	15.2	New obs. (2008); Hallot (2010)
66	Ton	Virton (L6440)	89	6.5	New obs. (2007)
67	Ton	Harnoncourt (L5520)	293	27.6	New obs. (2008)
68	Vire	Ruette (L5600)	104	21.3	DCENN/SPW and new estimate (2009)
69	Vire	Latour (L6030)	125	12	New obs. (2008)
BRABANT PLATEAU					
70	Senne	Quenast (~L5660)	169	19.5	New obs. (2011)
71	Dyle	Florival (L6160)	430	20.5	New obs. (2011)
72	Samme	Ronquières (S2371)	135	15	Denis et al. (2014)

NB: Site locations with double values (#4, #11, #20, and #58) are those where suspended sediment samples were taken with no gauging station nearby. Discharge values of the closest station have been used instead

The average percentage of cultivated area greatly varies with the region where the studied watersheds are located: 19% in Ardenne, 30% in Entre-Vesdre-et-Meuse, 37% in Fagne-Famenne, 28% in Lorraine, 54% in the Condroz, 50% in the Brabant Plateau, 49% in the Haine basin, and 75% in Hesbaye, based on the Corine Land Cover map of 2006. Conversely, the average forested area ranges from 2% in Hesbaye to 55% in Ardenne.

2.2 Field sampling

2.2.1 Sampling methods

To estimate the concentration of wash load and suspended sediment, a manual sampling methodology was set up to allow a large number of sampling sites during flood periods, with the sampling of a bucket of 5 l of river water from a
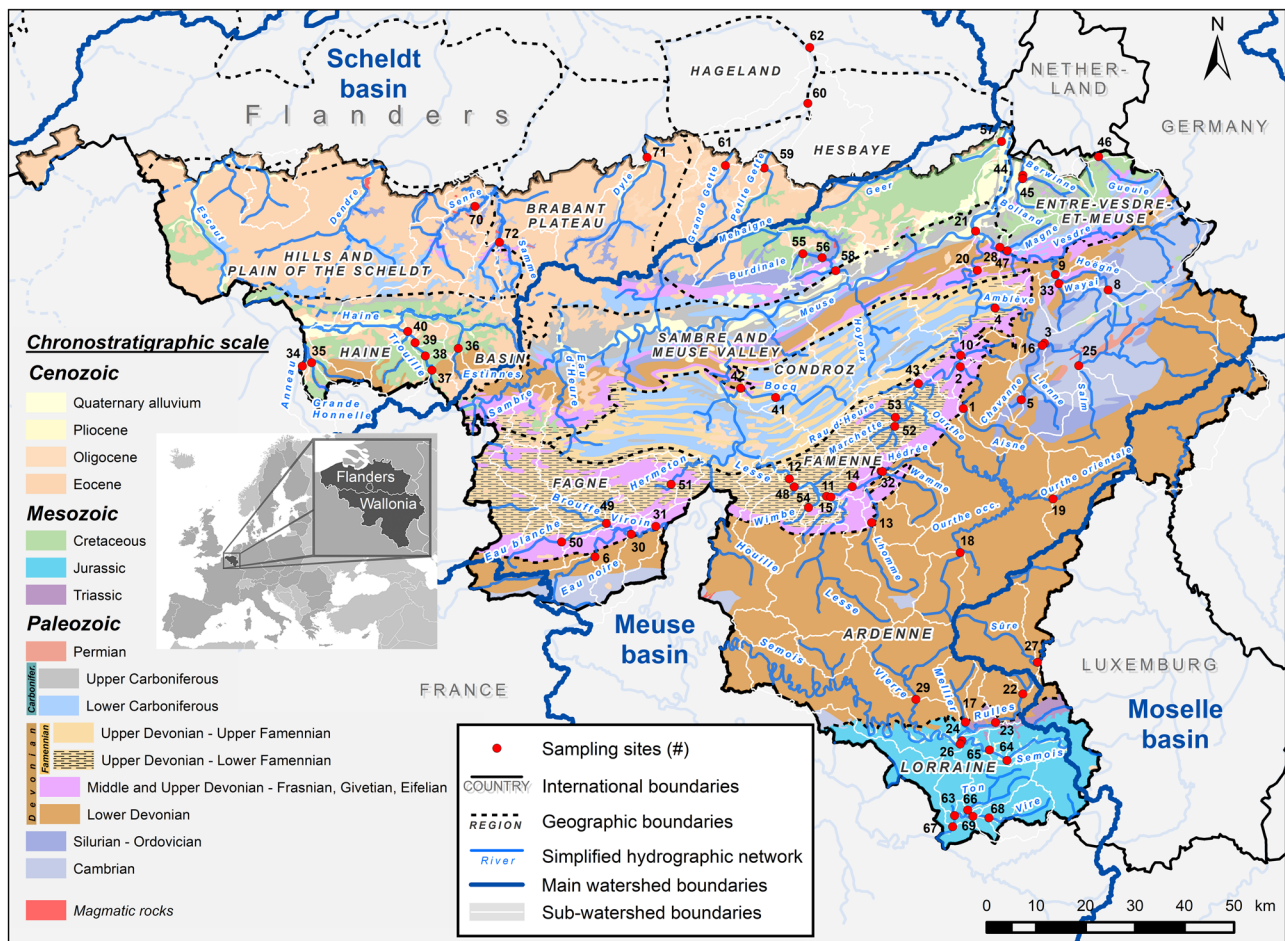
Fig. 1 Location of sampling sites and simplified geological map of Wallonia (according to de Bethune (1954) and Dejonghe (2007), modified). Station numbering refers to Table 1. The sub-watershed area of each river studied is shown with its appurtenance to the main basin (Scheldt, Meuse, and Moselle)

bridge in the centre of the river. This method was chosen for its speed of implementation (Lemin et al. 1987) and its efficiency in obtaining reproducible results with different operators. Between 1994 and 2002, 250 samples were taken during fieldwork for academic research master theses (Perpinien 1998; Hombrouckx 2002; Monseur 2005). The

Table 2 Regional affiliation of each station in terms of lithology and loess availability

#	Region	Geological substratum and loess availability
#1 to #33	Ardenne	Impervious schisto-sandstone substratum of Cambrian-Ordovician and lower Devonian formations
#34 to #40	Haine Basin	Meso-Cenozoic sediments accumulated in an actively subsiding area, with Cretaceous chalk formations surmounted by Eocene sands, covered by a thick layer of loess
#41 to 43	Condroz	Appalachian structure with Carboniferous limestone formations in depressions and Upper Devonian sandstone formations on its ridges
#44 to #47	Entre-Vesdre-et-Meuse	Devonian rocks, Cretaceous deposits and Meuse terraces area, with gravel-bed rivers on moderately permeable substrates
#48 to #54	Fagne and Famenne	Lithological depression eroded into the lower Famennian and Frasnian soft shales
#55 to #62	Hesbaye	Cretaceous chalk covered by several metres of loess
#63 to #69	Lorraine	Sandy-loaded rivers developed on Triassic and Lower Jurassic deposits of various kinds: marl and sandstone, limestone, and sandy limestone
#70 to #72	Brabant Plateau	Cambrian-Ordovico-Silurian formations under sandy Eocene and loessic cover

representativeness of the results obtained with this sampling method has been validated across the cross section of several rivers in Wallonia (Pironet 1995; Monseur 2005). After this first phase of samplings, around 1300 samples were taken between 2003 and 2010. Then 450 samples were collected in the 2010–2016 intervals. The average number of samples per study site was 40, with a coefficient of variation of 1.76. Over the whole dataset, 25% were taken in rising limbs, 24% in recession limbs, with different and independent events, and the other 51% were sampled during almost constant flow rates between floods. Recent reproducibility tests (2011–2014) were performed in the watersheds of the Gette, Senne, and Dyle rivers in order to validate the method of systematic subsurface sampling at the point where the flow is the fastest, according to the morphology of the stream bed (Van Campenhout et al. 2013).

2.2.2 Hydrologic series availability

Computing median sediment yield over years needs discrete or continuous water concentration sampling and the recording of discharge data at the same gauging station. With the aim of comparing sediment transport from different geographical regions, and due to the variability of SSY, computations of median SSY at gauging stations have to be compared over the same period of time in order to have consistent results. Discharge data from the dataset do not cover the same period at each location because their installation date varies. Figure 2 gives information about the mean

number of days per year where discharge is above bankfull discharge (Q_b), which has been observed in the field or computed from partial series with the methodology of Van Campenhout et al. (2020). Figure 2 also shows the number of stations with at least 90% of hourly discharge data available for a given year. Median SSY will be computed from annual SSY interpolated data in the 1996 to 2018 intervals. This time span maximizes the availability of discharge data over most of the monitored stations, and is consistent with the sampling period.

2.3 Laboratory analysis of the suspended sediment particles

The concentration of suspended solids is measured by vacuum-filtering the samples with 110-mm diameter Whatman GF/C glass microfibers filters — mesh = 1.2 μm (Smith 2007) with 98% retention efficiency (Zimmermann et al. 2012). These filters allow working with the huge concentrations that can be attained in loamy rivers (up to 20 g l^{-1}) and are compatible with Loss On Fire procedure. The methodology is based on the NF EN 872–2005 standard (Marttila and Kløve 2010). The accuracy of the measurements depends on the mass of the sediment-filled filter. Tests performed on precisely known mass and volume samples indicate an error of the order of 10% for samples < 100 mg l^{-1}, of the order of 5% for samples of 500 mg l^{-1}, and the order of < 2% for samples of 2000 mg l^{-1}. Concentration values ≤ 10 mg l^{-1} were rejected due to the uncertainty, representing ~ 8% of samples.
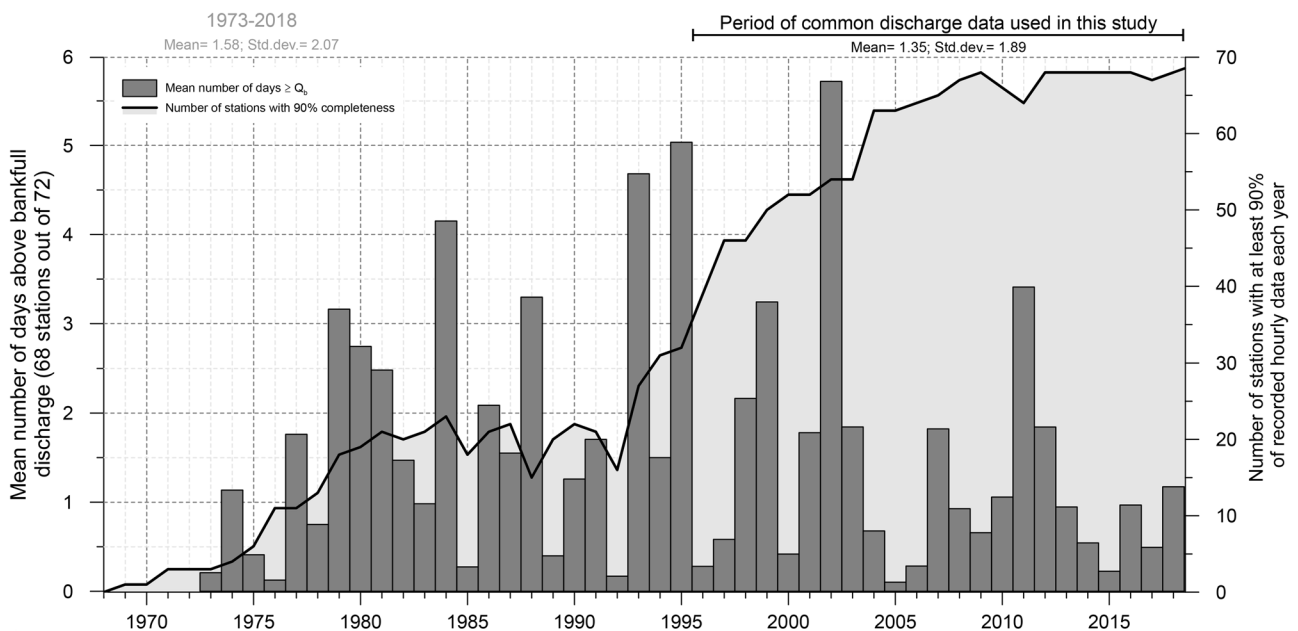

Fig. 2 Average number of days above bankfull discharge (Q_b) for studied gauging stations, availability, and representativeness of hydrologic data

2.4 Sediment yield computations

2.4.1 Rating curves and logarithmic corrections

Water sampling strategies and sediment load calculation are crucial to provide accuracy and reliability in results. Interannual variability of sediment load complicates the mid- and long-term estimations of the sediment yield (Syvitski et al. 2000). The sampling strategy used in our study was set up as a first-line approach to obtain sediment transport data for gauging stations that had never been the subject of suspended sediment studies in Wallonia. While many fluvial systems show a non-linearity behaviour in the relationship between discharge and sediment concentration and high uncertainty related with non-continuous monitoring (Webb et al. 1997; Araujo et al. 2012), sampling campaigns were first made to obtain flood water samples related to real-time water level alerts. These flood water samplings were augmented by other samples taken during recessions and low water periods. The sampling regimen was, at most, one sample per station per event in order to prevent intra-event correlation. The campaigns lasted for at least 5 years in order to cover as thoroughly as possible the observed discharges, from low water to above bankfull discharge.

The instantaneous concentration of suspended solids (C_s) in a river with well homogenised flow is commonly related to the instantaneous flow rate (Q) by a power function (Eq. 1), better known as the sediment rating curve (Campbell and Bauder 1940), where a and b are two empirical constants (Phillips et al. 1999; Meybeck et al. 2003; Li et al. 2005; Rovira and Batalla 2006; Doomen et al. 2008; Delmas et al. 2011).

$$C_s = aQ^b \tag{1}$$

C_s is generally expressed in mg l^{-1} and Q in m^3 s^{-1}. Parameters a and b are computed by least squares regression in logarithmic space formed by log C_s/log Q from measured concentration and discharge values.

A key factor of the sediment rating curve is its statistical significance. The coefficient of determination (R^2) of the curve, the standardized root-mean-squared error (RMSE),

referred to as RSR (RMSE-observations standard deviation ratio, Eq. 2), the Nash–Sutcliffe efficiency coefficient (NSE, Eq. 3), and the percent of bias (PBIAS, Eq. 4) have been computed following the equations presented by Jung et al. (2020) based on Moriasi et al. (2007) and shown in Table 3.

$$\text{RSR} = \frac{\text{RMSE}}{\sigma_{obs}} = \left[\frac{\sqrt{\sum_{i=1}^{n} (C_i^{obs} - C_i^{est})^2}}{\sqrt{\sum_{i=1}^{n} (C_i^{obs} - C_i^{mean})^2}} \right] \tag{2}$$

$$\text{NSE} = 1 - \left[\frac{\sum_{i=1}^{n} (C_i^{obs} - C_i^{est})^2}{\sum_{i=1}^{n} (C_i^{obs} - C_i^{mean})^2} \right] \tag{3}$$

$$\text{PBIAS} = \left[\frac{\sum_{i=1}^{n} (C_i^{obs} - C_i^{est}) * 100}{\sum_{i=1}^{n} (C_i^{obs})} \right] \tag{4}$$

Equations 2, 3, and 4 give the RSR, NSE, and PBIAS calculations, respectively, where RMSE is the root-mean-squared error, σ_{obs} is the standard deviation of the observed concentrations, C_i^{obs} is the observed concentration, C_i^{est} is the estimated concentration for the same index i, and C_i^{mean} is the mean SSC observed concentration from n observations. The values of the NSE can range from $-\infty$ to 1 (optimal value), where value between 0 and 1 are acceptable, and those values smaller than 0 are not considered as usable. The PBIAS measures the tendency of the estimated concentrations to be higher or lower than the observed data (Jung et al. 2020). The value of RSR varies from the optimal value of 0, which indicates zero RMSE or residual variation and therefore perfect model simulation, to a large positive value. The lower the RSR, the lower the RMSE, the better the model simulation performance (Moriasi et al. 2007). The validation criteria are shown in Table 3, with modifications compared to Jung et al. (2020) because they use an additional constant

Table 3 Validation criteria of the sediment rating curves, adapted from Jung et al. (2020)

	RSR (RMSE-observations standard deviation ratio)	NSE (Nash–Sutcliffe efficiency coefficient)	PBIAS (percent of bias)
Excellent	(0.00–0.25)	(0.75–1.00)	
Very good	(0.25–0.50)	(0.50–0.75)	< 10
Good	(0.50–0.75)	(0.25–0.50)	(10–30)
Satisfactory	(0.75–1.00)	(0.00–0.25)	(30–50)
Unsatisfactory	≥ 1.00	< 0.00	≥ 50

term p to Eq. 1 in order to take into account the non-linearity of the suspended sediment rating-curve. This would have needed a greater number of samples to be computed.

2.4.2 Spatial and temporal sediment yield calculation

At watershed scale, the specific annual sediment yield was computed as the sum, for each time interval, of the product of the instantaneous flow and the concentration of suspended solids estimated via Eq. 1 and discrete samples (Syvitski et al. 2000; Cerdan et al. 2012). This method of estimation is based on the hypothesis of a unique relationship between Q and C_s and on the assumption that an instantaneous C_s depends only on Q at any given time without hysteresis phenomena (Ritchie 2007; Cerdan et al. 2012). Not enough samples were collected in this study to differentiate flow conditions and obtain flood- and recession-sediment curves at each gauging station The method proposed by Ferguson (1986, 1987) has been used to correct the bias due to the logarithmic de-transformation on both axes, which is only effective when the residuals of C_s follow a log-normal distribution and C_s is a power function of Q (Asselman 2000). A corrective factor is applied to the total suspended and wash load estimations (Phillips et al. 1999), as shown by Eq. 5 to give the corrected daily mass of suspended and wash loads ($f_{daily\,corr.}$) from Q_h, the hourly discharge; C_h the estimate suspended sediment concentration, and with s, the standard error of the estimation of the least squares regression in $\log_{10}$ units.

$$f_{daily\mathrm{corr.}} = \sum_{h}^{24} 3600 Q_h C_h \exp(2.651 s^2) \tag{5}$$

2.5 Physical characteristics of the studied watersheds

The physical data of the watersheds have influence on soil erosion and sediment transport efficiency (Syvitski et al. 2000). These parameters have been extracted from the global 1-arcsecond (30-m) Shuttle Radar Topography Mission (SRTM) Digital Elevation Model (DEM) downloaded from the United States Geological Survey's EarthExplorer site (http://earthexplorer.usgs.gov). However, the mean slope of the watersheds may not be ideal to describe the runoff concentration time of the watershed. The Roche's slope index I_p, also called the index of runoff susceptibility and based on the compactness coefficient of Gravelius (1914), was computed for each watershed (Roche 1963). Additionally, the hypsometric curve (Davis 1899) and the hypsometric integral were computed for each (Table 8 in Supplementary Materials) watershed (Strahler 1952; Demoulin 2012).

2.6 Multi-criteria analysis on physical watershed variables

Correlation matrices will be used in the first approach in order to isolate the variables with the greater influence on the integrated value of sediment transport at the outlet. The physical variables that will be used are the watershed area, the mean elevation and slope, the Roche's slope index, and the hypsometric value, whilst the variables related to the land use will be the relative proportion of forests, grassland, and cultivated areas. The Corine Land Cover map that has been used is the reference year 2006 because a majority of samples were taken around 2006 (CORINE Land Cover 2018). Land cover maps of 2000, 2012, and 2018 will also be taken into account in the correlation analysis. In the second approach, weighted coefficients of these variables will be computed as well as the coefficient of multiple determination.

3 Results

3.1 Sediment rating curves analysis

The results of this study are presented in Table 4, which gives all the parameters that were computed from the water samplings and the computed SSY. The parameters 'a' (Fig. 3) and 'b' (Fig. 4) of the sediment rating curves were plotted in relationship with the watershed area and the regional affiliation of the stations. Even if lower 'a' values are observed in the Ardenne rivers and higher 'a' values in the Hesbaye rivers, no other obvious regionalization effect appears. The parameter 'b' does not show any relationship with the watershed area among the studied sites. However, when dealing with several stations on the same river, the parameter 'b' tends to increase with the drained area, while the parameter 'a' decreases with the watershed area.

Based on the validity criterion (Table 3), the unsatisfactory sediment rating curves are presented in Table 5. In addition to the validity criterion, a small number of stations hugely overpredict suspended sediment concentration based on maximum recorded discharge: #61 Grande Gette River at Sainte-Marie-Geest ($\sim$ 59 g l^{-1}) and #42 Bocq River at Yvoir ($\sim$ 35 g l^{-1}). All the other stations show peak concentrations below 17 g l^{-1}. For comparison, in a 134-km^2 watershed in the loess belt region (#59), automatic sampling far below the water surface during the rupture of a storm dam on 29 June 2011 led to measured concentrations around 25 g l^{-1}.

Table 4 Sedimentary parameters of the stations

#	River	Location	n[1]	Equation Cs = a Qb	R²	Estimated SSC at Q_b (mg l⁻¹)	Corrected SSY (1996–2018) (t km⁻² year⁻¹)				Years of Q_h data
							Mean	Median	Std.dev.	Min–max	
ARDENNE											
1	Aisne	Erezée (L6690)	28	5.9912 Q^0.9945	0.58	43	14	12.2	5	6.5–24.6	20
2	Aisne	Juzaine (L5491)	19	15.123 Q^0.7631	0.31	170	49.1	43.2	22.4	16.5–113	23
3	Amblève	Targnon (S6671)	15	0.4716 Q^1.2863	0.54	148	37.4	29.5	21.8	19.3–103.3	20
4	Amblève	Martinrive/Nonceveux (S6621)	14	0.0649 Q^1.7623	0.87	393	59.7	43.2	37	13.3–164.7	23
5	Chavanne	Vaux-Chavanne (ULiège data)	17	95.095 Q^1.3252	0.55	390	-	-	-	-	-
6	Eau Noire	Couvin (L6350)	11	1.702 Q^1.2714	0.68	140	25.7	19.2	18.3	4.0–70.9	22
7	Hédrée	Hargimont (L6940)	17	57.273 Q^0.4087	0.45	167	32.4	29.1	11.8	16–53.7	15
8	Hoëgne	Belleheid (S6526)	15	6.9513 Q^1.1015	0.61	88	24.2	20.2	12.3	10.5–50.8	23
9	Hoëgne	Theux (L5860)	94	1.6243 Q^1.2454	0.7	145	21.4	16	13.4	2.8–53.7	21
10	Lembrée	Vieuxville (L6300)	10	19.253 Q^1.0945	0.75	185	21.2	19.4	14	4.1–62.7	23
11	Lesse	Lessive (L6360+L5080)	14	11.241 Q^0.4925	0.34	87	31.7	28.1	9.8	17.8–52.7	20
12	Lesse	Hérock (L6610)	18	1.0149 Q^1.0905	0.73	162	36.9	30.7	20.2	14.9–86.7	22
13	Lhomme	Grupont (L6360)	15	5.8101 Q^1.0876	0.64	151	25.3	23.7	10.7	8.7–45.4	22
14	Lhomme	Rochefort (L6650)	21	9.8831 Q^0.6121	0.47	111	25	24.7	8.3	13.8–46.5	22
15	Lhomme	Eprave (L6360)	20	8.2648 Q^0.6460	0.42	116	27	24.2	9.5	12.3–46.2	23
16	Lienne	Lorcé (L6240)	20	11.096 Q^0.7821	0.31	121	47	40.8	39.6	13.9–199.1	23
17	Mellier	Marbehan (L5500)	19	2.7469 Q^1.0663	0.48	28	14.4	12.1	7.6	2.7–28.8	23
18	Ourthe occidentale	Amberloup (L6290)	8	7.1261 Q^0.7544	0.66	49	14.2	12.5	5.8	6.6–26.2	23
19	Ourthe orientale	Houffalize (L5930)	23	10.604 Q^0.8078	0.5	124	28.3	24.1	13.4	10.2–60.9	23
20	Ourthe	Méry Sauheid (S5857)	96	3.8371 Q^0.6031	0.22	118	35.3	30.3	12.8	12.7–67.8	23
21	Ourthe	Liège (Angleur) $Q_{Sauheid}+Q_{Chaudfontaine}$[2]	58	0.402 Q^0.9558 (Lemin 1984)	0.39	122	17.1	14.7	8	4.7–40.3	23
22	Rulles	Forêt d'Anlier[3]	21	76.225 Q^1.1999 (Petit 1983)	0.48	104	-	-	-	-	-
23	Rulles	Habay-la-Vieille (L5970)	24	3.687 Q^0.6906	0.3	19	7.9	7.3	3	2.4–12.9	23
24	Rulles	Tintigny (L5220)	23	5.0188 Q^0.5194	0.34	26	14.6	12.9	5.2	5.7–23.3	23
25	Salm	Trois-Ponts (L6070)	9	8.6214 Q^0.7219	0.49	85	28	22.9	14.1	7–66.4	23
26	Semois	Tintigny (S9561)	15	1.5613 Q^0.8486	0.45	36	11.9	10.4	4.5	4.8–22.1	15
27	Sûre	Martelange (L5610)	24+88	7.4284 Q^0.4554	0.34	36	13.4	11.9	5.2	4.9–26.9	23
28	Vesdre	Chaudfontaine (S6228)	32	3.0763 Q^0.8923	0.35	220	43	33.7	19.2	12.7–96.5	23
29	Vierre	Suxy (L7140)	15	3.8491 Q^0.7929	0.44	40	19.4	17.4	6.5	10.1–34.2	15
30	Viroin	Olloy-sur-Viroin (L6380)	14	3.157 Q^0.8300	0.56	88	35.9	26.4	23.8	10.9–95.1	23
31	Viroin	Treignes (L6760)	13	0.4589 Q^1.2495	0.69	80	20.6	17.9	11.9	9.4–52	11

Table 4 (continued)

#	River	Location	n^1	Equation Cs = a Qb	R^2	Estimated SSC at Q_b (mg l⁻¹)	Corrected SSY (1996–2018) (t km⁻² year⁻¹)				Years of Q_h data
							Mean	Median	Std.dev.	Min–max	
32	Wamme	Hargimont (old station L6370)	20	$4.797 Q^{1.1123}$	0.62	77	27.9	30.1	23.9	6.7–83.9	16
33	Wayai	Spixhe (L6790)	15	$22.958 Q^{0.8041}$	0.73	306	42.5	38.8	12.3	28.2–71.1	17
HAINE BASIN											
34	Anneau	Marchipont (L6870)	11	$80.762 Q^{1.7207}$	0.76	2,470	40.8	34.3	24.6	6.5–96.6	15
35	Grande Honnelle	Baisieux (L5170)	11	$23.491 Q^{1.4701}$	0.9	951	40.9	26.2	40	4.3–180.1	23
36	R^au des Estinnes	Estinnes-au-Val (L7080)	11	$243.21 Q^{1.4784}$	0.85	1,234	40.2	16.9	73.6	1.3–298.2	15
37	Trouille	Givry (L6710)	11	$100.05 Q^{1.8918}$	0.75	1,511	63.3	16.4	113.6	2.1–460.6	18
38	Trouille	Harmignies (L6430)	14	$26.746 Q^{2.1786}$	0.62	578	80.5	35.1	130.9	2.5–622.6	23
39	Trouille	Spiennes (L6600)	13	$32.566 Q^{2.3308}$	0.85	645	53.2	20.2	96	0.7–453.1	23
40	Trouille	Hyon (S3643)	12	$13.147 Q^{1.8394}$	0.84	733	51.2	28.4	50.5	5.7–186.8	23
CONDROZ											
41	Bocq	Spontin (L7320)	8	$12.23 Q^{1.624}$	0.46	1,373	62.5	42.7	86.8	9.4–400.4	23
42	Bocq	Yvoir (L5800)	10	$2.0462 Q^{2.4981}$	0.72	7,213	163.8	61.1	352.8	4.4–1643.3	23
43	Somme	Petite-Somme (ULiege data)	50	$44.739 Q^{1.0313}$	0.77	187	-	-	-	-	-
ENTRE-VESDRE-ET-MEUSE											
44	Berwinne	Dalhem (L6390)	43	$49.999 Q^{0.8793}$	0.46	604	68.1	58.7	35	24.1–133.7	23
45	Bolland	Dalhem (L6770)	36	$258.35 Q^{1.1923}$	0.55	1,111	77.2	74.8	30	30.3–123.9	23
46	Gueule	Sippenaeken (L6660)	30	$21.897 Q^{1.1337}$	0.72	508	44.3	38.2	22.6	17.9–93.1	-
47	Magne	Prayon/Foret (L6780/L7600)	30	$101.08 Q^{0.6635}$	0.31	282	40.6	36	24	8.2–94.3	23
FAGNE-FAMENNE											
48	Biran	Wanlin (L7190)	15	$47.699 Q^{0.4877}$	0.61	117	16.6	13.6	8.1	4.4–31.1	14
49	Brouffe	Mariembourg (S9111)	11	$12.91 Q^{0.8615}$	0.49	171	20.9	18.6	10.3	6.6–50.1	23
50	Eau Blanche	Aublain (L6530)	13	$9.8644 Q^{0.8787}$	0.74	119	20	18	9.3	3–42.1	19
51	Hermeton	Romedenne (L5060)	8	$21.392 Q^{0.8263}$	0.64	226	46.2	37.1	30.4	15.2–152.6	23
52	Marchette	Marche-en-Famenne (L7120)	13	$54.538 Q^{0.4606}$	0.19	135	30.2	25.2	11.5	19.8–56.8	15
53	R^au d'Heure	Baillonville (L6050)	22	$119.17 Q^{0.5229}$	0.6	474	74.2	64.1	31.4	40.3–165.3	23
54	Wimbe	Lavaux-Sainte-Anne (L6270)	16	$35.467 Q^{0.4583}$	0.45	123	22.1	21.7	8.4	9–35.8	23
HESBAYE											
55	Burdinale	Lamontzée[4]	93	$493.174 Q^{0.919}$	0.44	402	-	-	-	-	-
56	Burdinale	Marneffe (L6461)[5]	93	$574.116 Q^{1.271}$	0.67	1,564	32.9	19.1	27.8	4.9–80.7	10
57	Geer	Eben-Emael (L6340)	24	$16.49 Q^{2.0461}$	0.66	2,618	33.7	33.9	18.1	11.6–80.4	23
58	Mehaigne	Wanze (L5820)	94	$5.6674 Q^{2.0292}$	0.66	763	74.7	40.6	97.2	8.2–438.9	23
59	Petite Gette	Opheylissem (L6280)	76	$455.44 Q^{1.154}$	0.54	2,783	90.9	73.8	59.9	30–294.7	23

Table 4 (continued)

#	River	Location	n^1	Equation Cs = a Qb	R²	Estimated SSC at Q_b (mg l⁻¹)	Corrected SSY (1996–2018) (t km⁻² year⁻¹)				Years of Q_h data
							Mean	Median	Std.dev.	Min–max	
60	Petite Gette	Zoutleeuw (L09_154)[6]	113	$25.704\,Q^{2.8782}$ (Hombrouckx 2002)	0.22	3,123	81.9	80.3	40.8	20.6–168.6	23
61	Grande Gette	Sainte-Marie-Geest (L5720)		$166.3\,Q^{2.054}$	0.81	14,150	257.8	95	503.5	22.1–2422.4	22
62	Gette	Halen (L09_152)	92	$4.361\,Q^{1.6215}$ (Hombrouckx 2002)	0.59	460	23.5	18.8	16.1	6.7–64.2	23
LORRAINE											
63	Chavratte	Dampicourt (L7060)	8	$30.668\,Q^{1.0122}$	0.73	74	10.9	11.5	3.1	5.8–15.4	14
64	Semois	Chantemelle (L5880)	20	$9.7739\,Q^{0.6329}$	0.62	45	10.1	9.7	3.4	4.8–16.2	23
65	Semois	Etalle (L6180)	21	$9.6593\,Q^{0.5570}$	0.5	44	13.7	13.8	4.5	7.7–20.8	23
66	Ton	Virton (L6440)	11	$11.396\,Q^{1.4461}$	0.81	171	14.6	13.3	6.6	8.5–34.3	23
67	Ton	Harnoncourt (L5520)	17	$6.5632\,Q^{0.9897}$	0.49	175	24.6	21.9	11.4	8–55.6	23
68	Vire	Ruette (L5600)[7]	15	$10.601\,Q^{1.2609}$	0.69	502	33.4	31.1	18	5.3–65.2	23
69	Vire	Latour (L6030)	12	$10.966\,Q^{1.1516}$	0.68	192	33.4	22.6	15.6	7.8–66.1	23
			15								
BRABANT PLATEAU											
70	Senne	Quenast (~L5660)	473	$69.861\,Q^{1.3421}$	0.75	3,763	268.8	203.4	269.3	20.9–1031.5	23
71	Dyle	Florival (L6160)	370	$1.6353\,Q^{2.7705}$	0.62	7,044	115.5	109.6	73.1	43.4–275.2	21
72	Samme	Ronquières (S2371)	133	$42.38\,Q^{1.3}$	0.71	1,432	49.8	43	39.2	14.6–196	23

[1] n is the number of samples per station

[2] The samples taken by Lemin et al. (1987) in Liege covered the period 1983–1984

[3] The samples taken by Petit (1983, 1987) covered the period 1975–1977

[4] The station of Lamontzée on the Burdinale River uses data collected by Lamalle (1987) with samples taken in 1986. The sediment yield was estimated at 48 t km⁻² year⁻¹ in 1986

[5] The station located in Marneffe on the Burdinale River uses data collected by Lamalle (1987) with samples taken in 1986. The sediment yield was estimated at 89 t km⁻² year⁻¹ in 1986

[6] The station of Zoutleeuw on the Petite Gette River is based on samples collected by Hombrouckx (2002) in 2001–2002

[7] Station #69 (Vire at Latour) uses in addition sampling data from Ruette to optimize the rating curve because their watershed areas and their sediment transport behaviour are similar
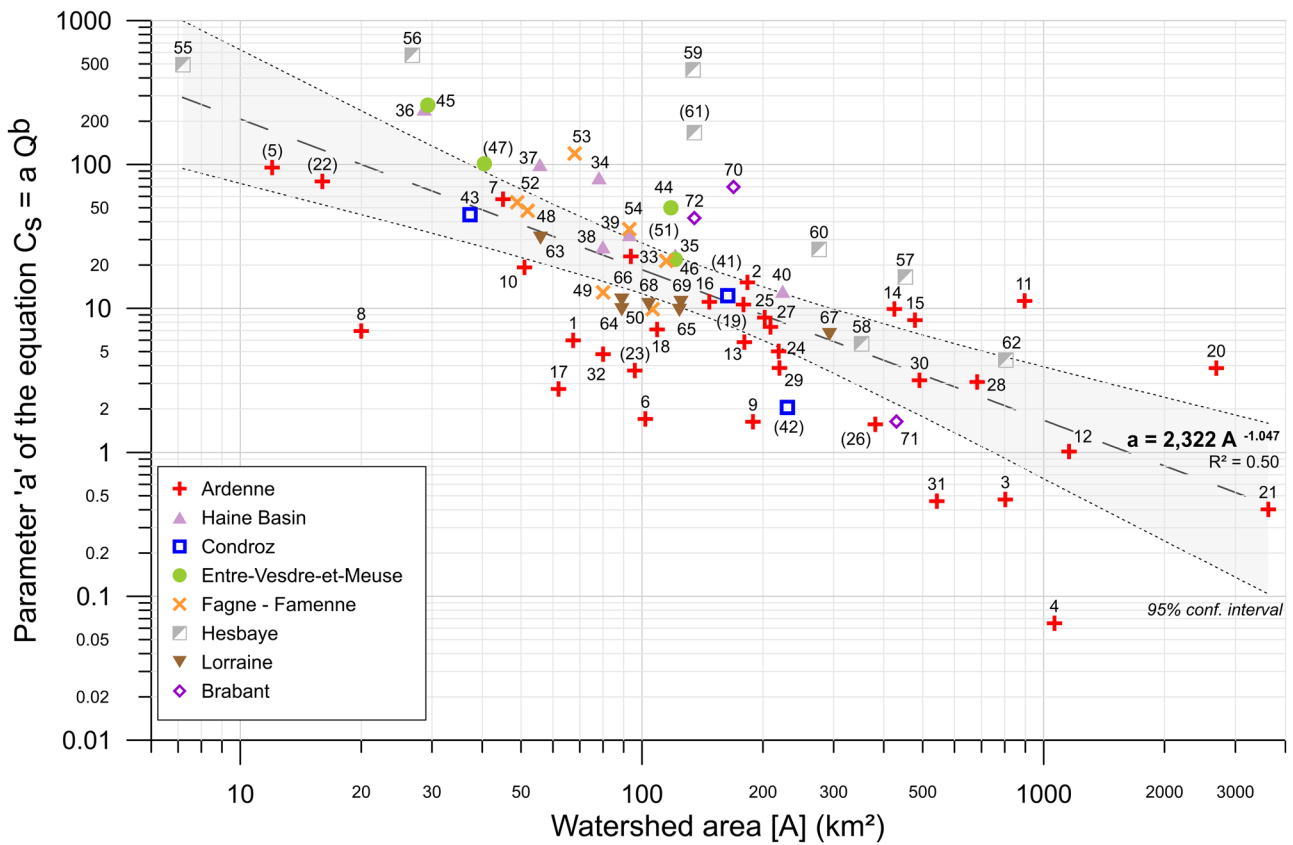
Fig. 3 Relationship between the parameter '*a*' of the rating curve equation $C_s = a\,Q^b$ and the watershed area with a regionalized differentiation. The values between brackets stand for the sediment rating curves considered as unsatisfactory

3.2 Spatial and temporal specific sediment yield variability analysis

Through the computation of sediment rating curves and the hydrological series, the annual sediment transport at the stations was calculated. Due to the significant temporal variability of annual sediment yield, which is directly linked to the variability of rainfall and river flows, the average and the median annual sediment yields during the 1996–2018 period were computed (Table 4) and the median SSY values were mapped (Fig. 5). The overall weighted-area median SSY was 32.7 t km^{-2} year^{-1}, taking into account the 58 valid stations. The median sediment yield for the period 1996–2018 reveals clear regional variability. Considering the computed data for valid sediment rating curves (therefore without the unsatisfactory stations), the median SSY reaches, on average, 19.2 t km^{-2} year^{-1} in Lorraine, 24.9 t km^{-2} year^{-1} in Ardenne, 26.9 t km^{-2} year^{-1} in the Haine basin, 28.4 t km^{-2} year^{-1} in Fagne-Famenne, 41.4 t km^{-2} year^{-1} in Hesbaye, 49.2 t km^{-2} year^{-1} in Entre-Vesdre-et-Meuse, and 119.0 t km^{-2} year^{-1} in the Brabant Plateau. The annual sediment yield is very dependent upon the annual runoff and the intensity of the floods. Regional differences were

observed in relationship to the proportion of agricultural areas, the availability of fine sediment, and to a less extent, the slope of the watershed in a runoff concentration time point of view.

The region with the most marked median SSY (Hesbaye and Brabant Plateau) also shows the most marked annual variation. In Hesbaye, the studied watersheds belong to two large watersheds: the Meuse basin and the Scheldt basin. The median SSY of the rivers belonging to the Scheldt basin (Petite Gette and Grande Gette rivers) is much higher than the values observed in the Meuse basin (Geer and Mehaigne watersheds). In the Brabant Plateau region and in the Senne watershed, SSY values tend to be even more important than in the Hesbaye region. The Entre-Vesdre-et-Meuse rivers tend to present large annual variations. The other studied regions show less marked annual and spatial variations. Rivers from the Haine basin (16 to 35 t km^{-2} year^{-1}) and the Fagne region (18 to 37 t km^{-2} year^{-1}) show lower median SSY values. These values in Fagne are understandable given the grassland which is the predominant land cover and the low slope of the watersheds. However, in the case of the tributaries of the Haine River, it seems that the type of flow — a predominant base flow while Ardennian rivers often show a
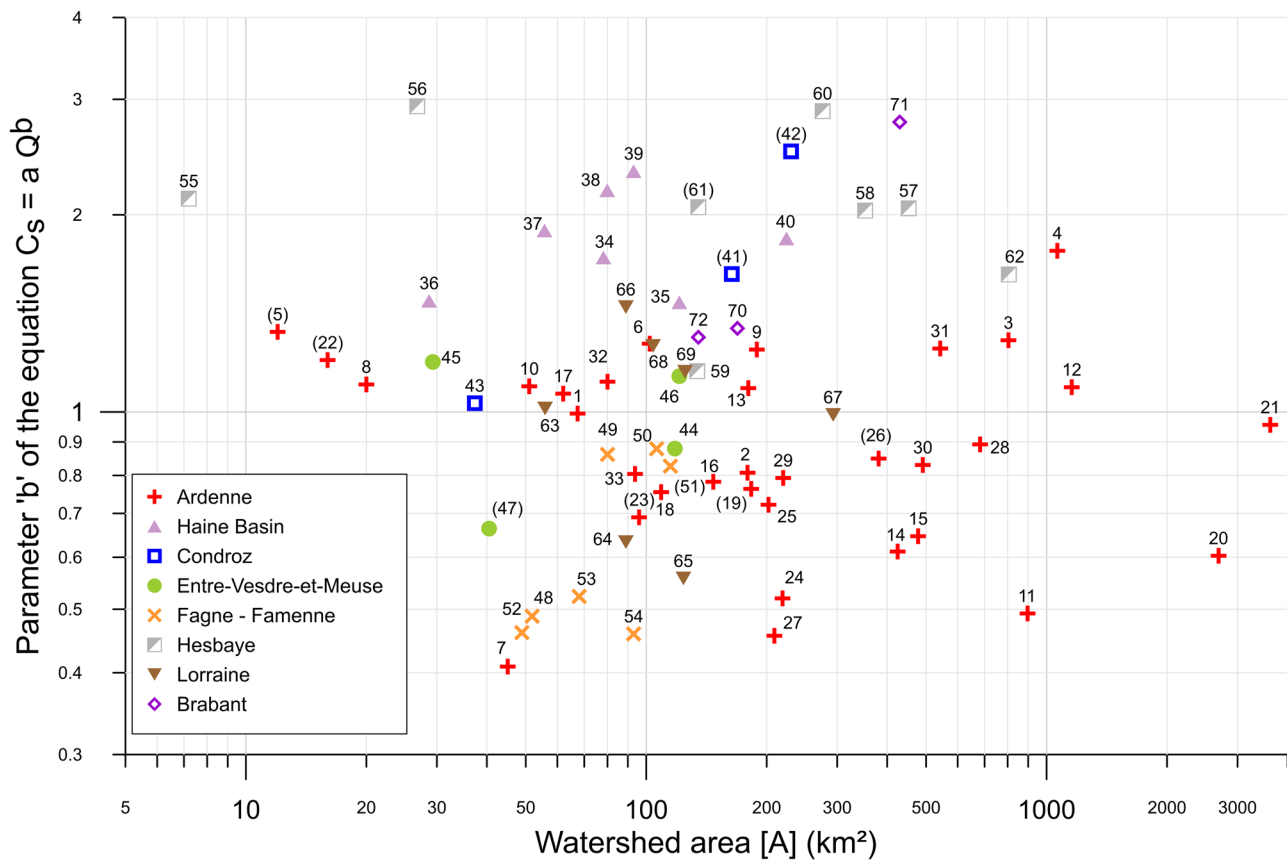
Fig. 4 Relationship between the parameter '*b*' of the rating curve equation $C_s = a\,Q^b$ and the watershed area with a regionalized differentiation. The values between brackets stand for the sediment rating curves considered as unsatisfactory

more flashy discharge regime — tends to explain the lower SSY value. In Famenne, the interannual variability is lower for the studied stations due to a smaller proportion of agricultural areas, preventing high sediment concentrations after summer storms, compared to the large plots in Hesbaye. The Lesse and the Lhomme rivers are subject to karstic losses at the interface of the Ardenne and the Famenne regions. Hart and Schurger (2005) showed that karstic zones can also behave like sedimentary sources, when floods re-suspend old deposits trapped within these cavities.

The median SSY of the rivers of the Ardenne region show, at first sight, a certain variability. However, the order of magnitude of these values agrees with the measurements made by estimating the sedimentary volume trapped by the Bütgenbach dam on the Warche River ($A = 72$ km^2), in a similar lithological and land use context than the upper Amblève River watershed where samples were taken (#3 Amblève River in Targnon, 803 km^2). Rivers from the southern part of the Ardenne region and the Lorraine region show lower SSY, due to the forestry and the grassland land cover respectively.

Due to the very high interannual variability of SSY, we analysed 2 years, i.e., 2002, representing a humid year

(Fig. 7 in Supplementary Materials), and 2018, representing a dry year (Fig. 8 in Supplementary Materials). Table 5 gives the average SSY by region for the humid and dry years in terms of days $> Q_b$, taking into account valid sediment rating curves. In the case of the humid year and even if the number of flood events and their intensity play a role, the Lorraine and Ardenne regions present quite low sediment transportation in comparison to the other regions. Entre-Vesdre-et-Meuse and Fagne-Famenne regions present intermediate results (~ 100 t km^{-2} year^{-1}). The larger SSY are observed in the Haine Basin, and above all in the Brabant Plateau and Hesbaye regions. These watersheds from the loess belt have greater availability of fine sediment to transport. In the case of long period of intense floods, SSY can exceed 300 to 600 t km^{-2} year^{-1}. The Senne River showed a SSY value of 1032 t km^{-2} year^{-1} but is still considered as a valid value in terms of maximum extrapolated concentration (9.3 g l^{-1}), contrary to the station #61, the Grande Gette River. Years with heavy runoff are those that contribute the most to sediment transport but uncertainties in SSY calculations are more important in the case of above-bankfull discharge and especially when extreme floods occur.

Table 5 Sampling representativeness

#	River	Location	Max. observ. discharge 1996–2018 ($m^3\ s^{-1}$)	Max. sampled discharge ($m^3\ s^{-1}$)	Max. extrapolated concentration (1996–2018) ($mg\ l^{-1}$)	R^2	RSR (RMSE-observations standard deviation ratio)	NSE (Nash–Sutcliffe efficiency coefficient)	PBIAS (percent of bias)	Sediment rating curve validity[1]
1	Aisne	Erezée (L6690)	21.85	9.90	129	0.58	0.87	0.24	48.0	Satisfactory
2	Aisne	Juzaine (L5491)	68.27	28.14	380	0.31	0.93	0.14	37.7	Satisfactory
3	Amblève	Targnon (S6671)	240.96	127.09	546	0.54	0.67	0.55	25.9	Good
4	Amblève	Martinrive/Nonceveux (S6621)	293.37	190.17	1447	0.87	0.84	0.29	12.8	Good
5	Chavanne	Vaux-Chavanne (ULiege data)	-	2.78		0.55	0.76	0.42	52.0	**Unsatisfactory**
6	Eau Noire	Couvin (L6350)	95.38	36.86	559	0.68	0.77	0.40	17.2	Good
7	Hédrée	Hargimont (L6940)	44.69	6.28	271	0.45	0.94	0.12	18.7	Satisfactory
8	Hoëgne	Belleheid (S6526)	24.50	10.48	236	0.61	0.77	0.41	33.7	Satisfactory
9	Hoëgne	Theux (L5860)	117.24	60.67	613	0.70	0.77	0.41	25.5	Good
10	Lembrée	Vieuxville (L6300)	24.33	19.74	633	0.75	0.70	0.51	20.2	Very good
11	Lesse	Lessive (L6360+L5080) Villers-sur-Lesse	202.89	119.93	154	0.34	0.96	0.07	15.5	Satisfactory
12	Lesse	Hérock (L6610)	291.60	116.20	495	0.73	0.83	0.31	17.2	Good
13	Lhomme	Grupont (L6360)	42.50	19.09	343	0.64	0.77	0.40	24.1	Good
14	Lhomme	Rochefort (L6650)	160.80	79.71	221	0.47	0.80	0.37	22.5	Good
15	Lhomme	Eprave (L6360)	126.06	108.68	188	0.42	0.92	0.15	17.2	Satisfactory
16	Lienne	Lorcé (L6240)	97.53	23.21	399	0.31	0.99	0.02	41.6	Satisfactory
17	Mellier	Marbehan (L5500)	43.08	23.68	152	0.48	0.95	0.09	17.6	Satisfactory
18	Ourthe occidentale	Amberloup (L6290)	20.05	14.89	68	0.66	0.99	0.02	8.3	Satisfactory
19	Ourthe orientale	Houffalize (L5930)	63.75	38.47	304	0.50	1.01	-0.03	30.0	**Unsatisfactory**
20	Ourthe	Méry Sauheid (S5857)	586.15	553.97	179	0.22	0.94	0.11	28.8	Satisfactory
21	Ourthe	Liège (Angleur) $Q_{Sauheid}+Q_{Chaudfontaine}$	684.34	562.30	206	0.39	0.88	0.23	32.8	Satisfactory
22	Rulles	Forêt d'Anlier	-	2.49	-	0.48	1.13	-0.28	14.5	**Unsatisfactory**
23	Rulles	Habay-la-Vieille (L5970)	32.96	24.15	41	0.30	1.01	-0.02	19.8	**Unsatisfactory**
24	Rulles	Tintigny (L5220)	55.84	46.62	41	0.34	0.97	0.06	25.1	Satisfactory
25	Salm	Trois-Ponts (L6070)	53.44	38.74	152	0.49	0.76	0.43	29.8	Good
26	Semois	Tintigny (S9561)	113.63	101.95	87	0.45	1.07	-0.14	14.8	**Unsatisfactory**
27	Sûre	Martelange (L5610)	88.45	43.78	57	0.34	0.94	0.11	28.9	Satisfactory
28	Vesdre	Chaudfontaine (S6228)	274.46	125.04	461	0.35	0.90	0.19	41.9	Satisfactory
29	Vierre	Suxy (L7140)	76.89	24.90	120	0.44	1.00	0.00	23.1	Satisfactory

Table 5 (continued)

#	River	Location	Max. observ. discharge 1996–2018 (m³ s⁻¹)	Max. sampled discharge (m³ s⁻¹)	Max. extrapolated concentration (1996–2018) (mg l⁻¹)	R^2	RSR (RMSE-observations standard deviation ratio)	NSE (Nash–Sutcliffe efficiency coefficient)	PBIAS (percent of bias)	Sediment rating curve validity[1]
30	Viroin	Olloy-sur-Viroin (L6380)	176.54	107.88	231	0.56	0.97	0.06	27.1	Satisfactory
31	Viroin	Treignes (L6760)	236.94	126.82	425	0.69	0.95	0.09	15.3	Satisfactory
32	Wamme	Hargimont (old station L6370)	34.01	23.45	242	0.62	0.72	0.48	25.7	Good
33	Wayai	Spixhe (L6790)	64.32	18.35	653	0.73	0.89	0.21	23.9	Satisfactory
34	Ameau	Marchipont (L6870)	12.75	6.71	6448	0.76	0.21	0.96	20.8	Very good
35	Grande Honnelle	Baisieux (L5170)	33.92	9.65	4177	0.90	0.24	0.94	10.4	Very good
36	R^{au} des Estinnes	Estinnes-au-Val (L7080)	15.45	2.02	13,922	0.85	0.60	0.64	28.9	Good
37	Trouille	Givry (L6710)	15.46	2.87	17,781	0.75	0.76	0.42	37.0	Satisfactory
38	Trouille	Harmignies (L6430)	13.53	5.44	7797	0.62	0.88	0.23	48.9	Satisfactory
39	Trouille	Spiennes (L6600)	9.65	5.72	6419	0.85	0.66	0.56	6.8	Very good
40	Trouille	Hyon (S3643)	29.06	14.75	6463	0.84	0.53	0.71	25.8	Very good
41	Bocq	Spontin (L7320)	39.12	4.46	4715	0.46	0.82	0.32	62.7	**Unsatisfactory**
42	Bocq	Yvoir (L5800)	49.42	11.00	**34,873**	0.72	1.21	-0.45	23.7	**Unsatisfactory**
43	Somme	Petite-Somme (ULiege data)	-	-	-	0.77	0.70	0.51	27.7	Good
44	Berwinne	Dalhem (L6390)	61.94	17.84	1882	0.46	0.86	0.26	27.5	Good
45	Bolland	Dalhem (L6770)	12.44	5.87	5219	0.55	0.64	0.59	24.5	Good
46	Gueule	Sippenaeken (L6660)	41.38	13.72	1491	0.72	0.66	0.56	19.9	Very good
47	Magne	Prayon/Foret (L6780/L7600)	30.94	2.88	985	0.31	1.01	-0.02	28.3	**Unsatisfactory**
48	Biran	Wanlin (L7190)	21.66	7.91	214	0.61	0.88	0.23	10.8	Satisfactory
49	Brouffe	Mariembourg (S9111)	48.60	27.62	366	0.49	1.00	0.00	15.8	Satisfactory
50	Eau Blanche	Aublain (L6530)	41.46	22.26	260	0.74	0.75	0.44	26.0	Good
51	Hermeton	Romedenne (L5060)	62.77	17.30	654	0.64	1.01	-0.02	39.2	**Unsatisfactory**
52	Marchette	Marche-en-Famenne (L7120)	23.12	8.73	232	0.19	1.00	0.00	26.0	Satisfactory
53	R^{au} d'Heure	Baillonville (L6050)	26.37	10.95	660	0.60	0.88	0.23	16.5	Satisfactory
54	Wimbe	Lavaux-Sainte-Anne (L6270)	27.88	15.11	163	0.45	0.73	0.46	13.6	Good
55	Burdinale	Lamontzée	-	2.63	-	0.44	-	-	-	-
56	Burdinale	Marneffe (L6461)	6.12	2.60	5741	0.67	-	-	-	-
57	Geer	Eben-Emael (L6340)	18.81	7.67	6680	0.66	0.58	0.67	16.3	Very good

Table 5 (continued)

#	River	Location	Max. observ. discharge 1996–2018 (m³ s⁻¹)	Max. sampled discharge (m³ s⁻¹)	Max. extrapolated concentration (1996–2018) (mg l⁻¹)	R²	RSR (RMSE-observations standard deviation ratio)	NSE (Nash–Sutcliffe efficiency coefficient)	PBIAS (percent of bias)	Sediment rating curve validity[1]
58	Mehaigne	Wanze (L5820) Moha	40.03	11.78	10,115	0.66	0.75	0.44	40.5	Satisfactory
59	Petite Gette	Opheylissem (L6280)	22.55	1.54	16,594	0.54	0.80	0.37	3.1	Good
60	Petite Gette	Zoutleeuw (L09_154)	7.73	6.31	9255	0.22	-	-	-	-
61	Grande Gette	Sainte-Marie-Geest (L5720)	17.43	9.14	**58,971**	0.81	0.83	0.31	15.2	**Unsatisfactory (max. conc.)**
62	Gette	Halen (L09_152)	28.30	23.15	986	0.59	0.52	0.73	9.7	Very good
63	Chavratte	Dampicourt (L7060)	4.01	3.30	125	0.73	0.68	0.54	3.2	Very good
64	Semois	Chantemelle (L5880)	22.84	15.24	71	0.62	0.90	0.19	14.0	Satisfactory
65	Semois	Etalle (L6180)	35.64	23.11	71	0.50	0.95	0.10	14.0	Satisfactory
66	Ton	Virton (L6440)	8.48	7.12	251	0.81	0.37	0.87	5.7	Very good
67	Ton	Harnoncourt (L5520)	48.29	31.96	305	0.49	0.99	0.01	22.1	Satisfactory
68	Vire	Ruette (L5600)	29.08	21.95	743	0.69	0.64	0.59	23.4	Good
69	Vire	Latour (L6030)	30.74	21.95	567	0.68	0.83	0.31	22.9	Good
70	Senne	Quenast (~L5660)	57.85	23.02	16,197	0.75	0.71	0.49	10.1	Good
71	Dyle	Florival (L6160)	25.58	18.48	13,007	0.62	0.86	0.25	19.2	Good
72	Samme	Ronquières (S2371)	-	-	-	0.71	-	-	-	-

[1]The sediment rating curve validity is based on the criteria RSR, NSE, and PBIAS shown in Table 3. If several criteria do not exhibit the same state of confidence, priority has been given to the NSE coefficient to define the validity state. The stations without values are those for which the pairs of points are not known (old academic works) or those without hydrological series
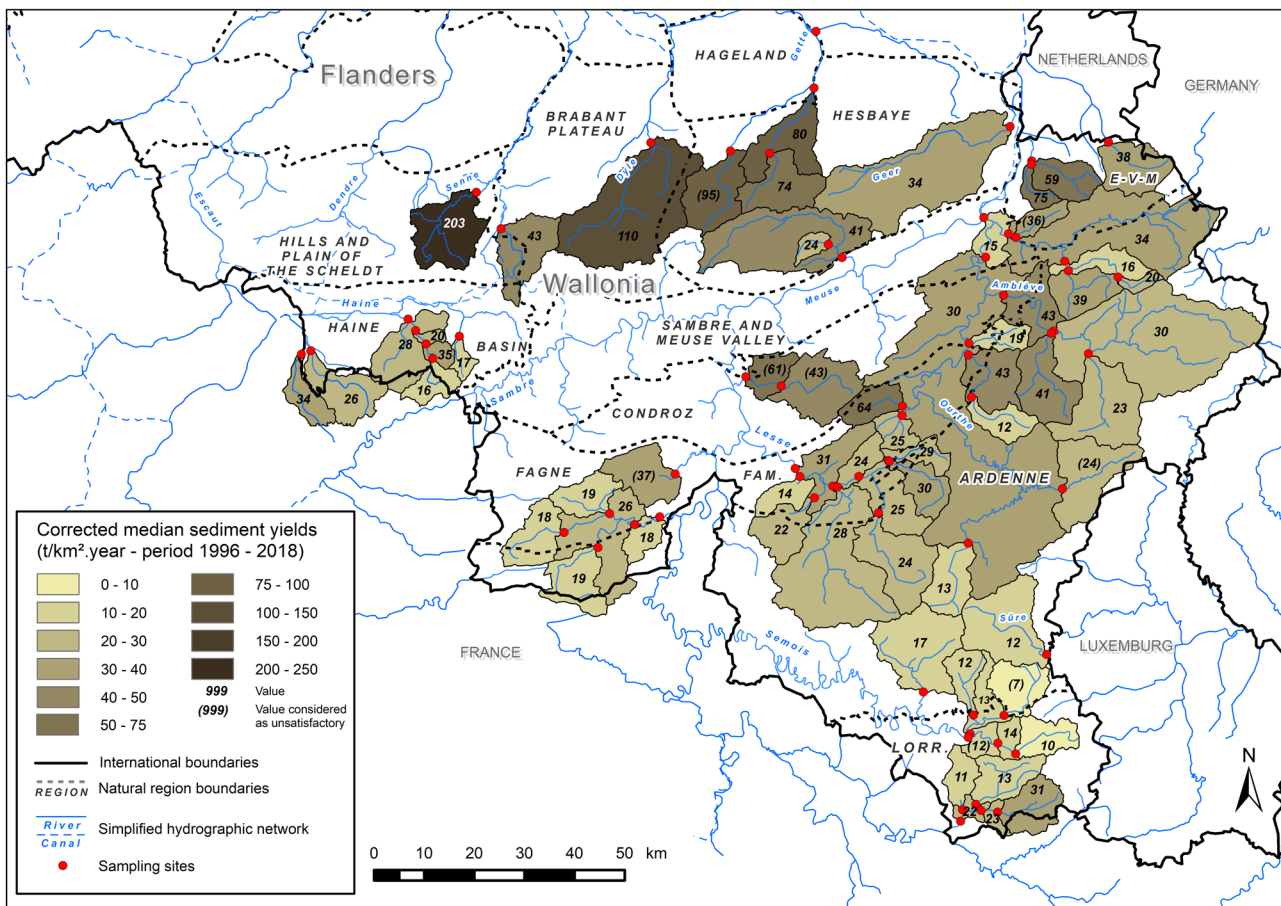
Fig. 5 Sediment yield median values within studied watersheds (period 1996–2018). Median SSY related to sediment rating curves that are considered as unsatisfactory are shown between brackets

The lowest annual discharge of the studied time interval was reached in 2018 in a vast majority of watersheds, although some significant flooding occurred in January and June. Figure 8 shows the average SSY values of 2018 taking into account only valid sediment rating curves and Table 6 presents the average values computed by region. In comparison to the year 2002, the year 2018 and its cumulative drought over a period of 3 years display great differences in terms of regional SSY values. The Haine basin presents the lowest SSY values, while this region was showing one of the highest SSY in a humid year. Ardenne and Lorraine regions present values pretty close to 2002 values. Fagne-Famenne region, for its part, has up to 5 times less SSY. Hesbaye and Brabant Plateau regions show around 10 to 20 times less SSY during a drought period. It should be noted that the Berwinne and Bolland watersheds, in Entre-Vesdre-et-Meuse, show very high SSY values, 131 t km^{-2} year^{-1} and 116 t km^{-2} year^{-1}, respectively. This is due to an intense thunderstorm accompanied by rainfall of 89 mm per day on 1 June 2018 in the town of Battice (headwaters of the Berwinne and the Bolland rivers). The

Berwinne River experienced flood discharge of 62 m^3 s^{-1} (recurrence ~ 120 years), while the Bolland River reached a flow rate of 12.4 m^3 s^{-1} (recurrence > 175 year). (Table 7)

3.3 Effects of physical characteristics of the watersheds on sediment yield

Table 1 gives the proportion of each type of land cover in the watersheds. Moreover, the sediment concentration at bankfull discharge has been used in order to compare rivers. This reference discharge has been selected because it is the most suitable discharge value to compare stations with each other. The recurrence of the bankfull discharge ($Q_{0.625}$ in partial series according to Van Campenhout et al. (2020) in the same geographical area) is usually in the range of sampled discharges. Comparison with greater floods (Q_2, Q_5, or Q_{10}) may lead to uncertainty due to the extrapolation of the sediment rating curve.

As a preamble to the analysis of regional differences in suspended sediment yield, some discrepancies in the relation between bankfull discharge and watershed area appears. The
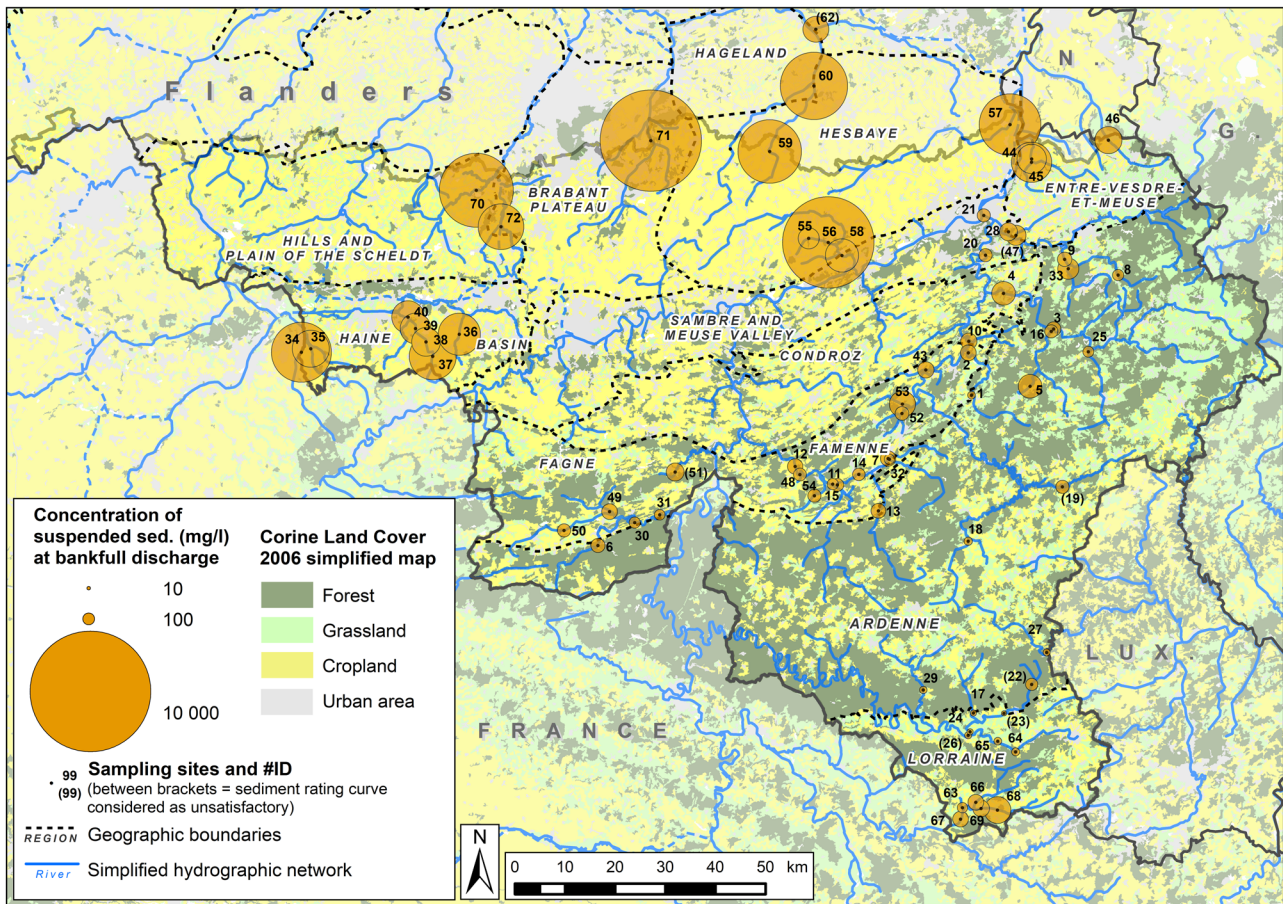
Fig. 6 Estimated suspended sediment concentrations at bankfull discharge and Corine Land Cover simplified map for 2006 (100-m resolution). Stations #41 and #42 were not shown because of their unrealistic SSC value at bankfull discharge

rivers located in the Haine Basin and those from the Hesbaye region clearly show Q_b values lower than the other rivers for a given value of watershed area (Petit and Pauquet 1997; Petit et al. 2007). In this case, it is more an influence of the hydrological regime, with a general weakness of the flows, rather than of the morphology of the bed and the size of the bed material (Petit et al. 2007). In the opposite case, with their soft-shale substratum that tends to increase the depth of the bed incision, Fagne and Famenne rivers show a higher bankfull discharge compared to the other rivers.

Ardennian rivers show less possibility of the accumulation of large alluvial plains, regarding their less important SSC at Q_b, unlike Brabant Plateau and Hesbaye rivers, with a large availability of loess. However, the rarity of overflowing floods prevents having a precise estimate of the concentrations of suspended sediment above Q_b. Some rivers in the southern part of the Lorraine region show local particularities, such as natural levees on the Ton River or an artificial dam in the Vire River, can induce, in the case of the Vire River, a significantly greater bankfull discharge value and thus, a greater sediment concentration at Q_b.

Figure 6 shows the estimated concentration at Q_b (see Table 4 for values). The variance of SSC is partially explained by the variance of Q_b ($R^2 = 0.60$), given by Eq. 6 (where SSC at Q_b is the suspended sediment concentration at bankfull discharge in mg l^{-1}, and $A_{a\%}$ is the proportion of agricultural area in the watershed expressed in percent).

$$SSC \ at \ Q_b = 38.72 A_{a\%}^{5.29} \tag{6}$$

Another important physical parameter is the mean slope of the watersheds: 4.2% in the Haine basin and in Hesbaye, 5.5% in the Brabant Plateau, 7.7% in Fagne-Famenne, 8.0% in Entre-Vesdre-et-Meuse, 8.9% in the Condroz, 9.8% in Lorraine, and 10.3% in Ardenne. It can be observed that slopes in central and south-western Ardenne are less steep than in the north-eastern Ardenne. The watersheds with the greatest average slopes are more likely to be forested. Inversely, the cultivated watersheds are prone to present the least steep slopes. However, local lower slopes in agricultural areas may lead to mudflows and flash-floods that contribute to higher sediment yield at the watershed integration

Table 6 Average SSY by region for 2002 (humid year) and 2018 (dry year)

Region	SSY in 2002 (t km^{-2} year^{-1})	SSY in 2018 (t km^{-2} year^{-1})
Ardenne	64.9	19.3
Haine Basin	380.6	12.2
Entre-Vesdre-et-Meuse	82.0	90.4
Fagne-Famenne	120.0	18.9
Hesbaye	636.4	36.3
Lorraine	30.1	23.4
Brabant Plateau	487.2	42.5

scale (Evrard et al. 2007; Van Campenhout et al. 2015). The Roche's slope index is given in Table 8 (see Supplementary Materials) and ranges from 0.045 to 0.197. It is a better representation of the overall slope of the watershed. The higher values of Roche's slope index (> 0.100) are observed in the watershed with an area that is lower than 200 km^2.

areas, and thus with the availability of suspended sediment runoff in the watershed. No correlation was found between the median SSY and the watershed area. For the duration of the water samplings, the land cover has not been drastically modified. However, some trends were detected in the studied watersheds (see Table 9 in Supplementary materials). From 2000 to 2018, the forest land cover has increased in all regions — and especially in Lorraine ($+0.9\%$) and Ardenne ($+0.4\%$) — except in Hesbaye and Entre-Vesdre-et-Meuse. Grassland tends to decrease in every region (up to -2.6% in the Haine Basin), except in Brabant Plateau and Entre-Vesdre-et-Meuse. Cultivated areas increase in the Haine Basin ($+1.8\%$) and in the Condroz ($+0.61\%$); they decrease especially in the Brabant Plateau region (-1.8%) and in Hesbaye (-0.9%). This decrease is related to the urbanization of the watershed ($+1\%$ in the loess belt). The Ardenne region is less marked by recent urbanization ($+0.2\%$). Multi-criteria analyses have been undertaken to extract the coefficients of the most correlated or inversely correlated variables with SSY (Eq. 7).

$$\text{Median SSY [t km}^{-2}\text{year}^{-1}] = 3.10 \text{ Mean slope[\%]} - 0.527 \text{ Forest cover [\%]}$$
$$+ 0.396 \text{ Cultivated cover [\%]} + 11.2$$

(7)

Correlation matrices have been used to detect the explanatory variables with respect to the median 1996–2018 specific sediment yields (Table 7). Despite our efforts to determine physical explanatory variables, only weak correlations between median SSY and land cover percentages are visible. The percentage of cultivated areas tends to be correlated with median SSY ($R = 0.42$), while the percentage of forested areas ($R = -0.45$) is inversely correlated with sediment yields. Physical variables that are linked to the relief energy show less meaningful correlations with median SSY. The mean slope of the watershed ($R = -0.28$) presents an inverse trend in comparison to the median SSY. The hypsometric value of the watershed showed a very weak correlation ($R = 0.21$) with median SSY. The mean elevation of the watershed is inversely linked with the median SSY ($R = -0.43$). However, the mean elevation is also related to the location of the agricultural

The coefficient of multiple determination (R^2) reaches a value of 0.48, with a standard error of 26.1 t km^{-2} year^{-1}. The multi-criteria analysis hardly explains the variance of median SSY with confidence, even if physical parameters of the watersheds play a role.

4 Discussion

The sediment rating-curve method tends to underpredict high and overpredict low SSC value (Horowitz 2003). Ideally, the calibration measurements should cover a full range of flow conditions from droughts to floods to ensure that extrapolation of the curve beyond the range of supporting measurements is minimized. However, achieving water sampling over a full range of flow rates

Table 7 Correlation between median SSY (1996–2018) and physical variables of the watersheds

Physical variables of the watersheds	Correlation (R) with median 1996–2018 SSY (t km^{-2} year^{-1})
Watershed area (A) (km^2)	−0.05
Mean elevation (m)	−0.43
Mean slope (%)	−0.28
Roche's slope index	−0.19
Hypsometric value	0.21
Forest relative land cover in 2006 (%)	−0.45
Grassland relative land cover in 2006 (%)	−0.21
Cultivated areas relative land cover in 2006 (%)	0.42

is difficult where the sampling site is remote from the lab or where the watershed is small so that the river has a quick response to infrequent storms. For this reason, some degree of extrapolation of the rating curve is often necessary (McKerchar 2003). In case of flash-floods or pluri-centennial floods, Keaton (2019) estimates the threshold between normal streamflow to hyperconcentrated sediment flow at a sediment concentration by volume of about 0.05 to 0.1 (50 to 100 g l^{-1}), while mud flood and mud flow are classified above 0.2 and 0.45 respectively. These reference values were used to ban the over-extrapolated values of the stations #42 and #61 (with about 35 and 59 g l^{-1} respectively); they are considered as unrealistic for their stream environment. In the end, the #62 station could be considered as invalid due to a probable underestimation of the sediment concentration (max. 986 mg l^{-1}) even if the NSE and PBIAS give a "very good" state of validity. There is a possibility that sediment accumulation occurred upstream of the sampling station according to Hombrouckx (2002). In any case, the manual sampling of over-bankfull discharges will remain hard due to the rarity of these events. Only automatic sampling stations would have achieved the gathering of data for very infrequent floods to study the within-event sediment variability and the hysteresis (Oeurng et al. 2010; Rodríguez-Blanco et al. 2010). In practice, this real-time monitoring and water sampling are rather difficult to set up in a large number of stations and requires high frequency field handlings and laboratory analyses.

Minimizing the sum of the squares of the logarithmic deviations results in the underestimation of the calculated concentrations (Wilson et al. 1990; Grasso and Jakob 2003; Hallot 2010). The bias increases with the degree of scatter about the regression (Ferguson 1986), despite the common use of a correction factor (Phillips et al. 1999; Ndomba et al. 2008), and the sediment yield underestimation may exceed 50% in some cases (Thomas 1985; Jansson 1985; Ferguson 1986, 1987; Koch and Smillie 1986; Cohn et al. 1989; Lamalle et al. 1989; Grasso and Jakob 2003). We have observed that the correction factor led to an increased value of around 30% when the R^2 of the sediment rating curve is around 0.5. In the case of a R^2 above 0.8, the increased value of the corrected SSY remains below 10%. The quality of the sediment rating curve has therefore a significant impact on the computed results, much higher than the exhaustiveness of the range of sampled discharges. However, the slope of the logarithmic rating curve could change significantly in case of new samples, because this type of mathematical relation is driven by extreme values. In addition, the values of the parameters 'a' and 'b' of the sediment rating curve may change with time: hydrologic changes may come from human-caused alterations of the global climate system or river restoration plans (Warrick 2015). Authors showed that variation in flow discharge can lead to a general decrease in 'b' and an increase in 'a' during the period with more flood events (i.e., an increase in sediment transport) and an increase in 'b' and a decrease in 'a' during droughts (Higgins et al. 2013).

The relationship between the SSY and the area of the watershed is rarely significant. In a large study of 60 watersheds in Spain, Verstraeten et al. (2003) could not explain more than 17% of the variability of the SSY with the watershed area. Multiple regression models, based on climatic, topographic, and land use properties, often are insufficient to model the sedimentary behaviour of the watersheds (Verstraeten et al. 2003). The same observations were made in Italy by de Vente et al. (2006). In the presence of clastic materials such as badlands, gullies, or landslides, the prediction of SSY seems to be easier, based on the drainage density (de Vente et al. 2006; Grauso et al. 2008). In Wallonia, the prediction seems to be more difficult due to the large range in the pattern of types of lithologies and soils over a rather small area. The high variability of lithologies prevents drawing a clear link between drainage density and sediment yield. The land cover is more likely to be used to explain a part of the spatial variability of sediment yields as it can be presented in correlation and multicriteria analyses. For instance, predominant agricultural land cover conjugated to higher watershed slope in the vicinity of the watercourses in the loess belt (Senne, Dyle and Gette rivers) is likely to explain higher SSY values.

From the samplings of this study, it was shown that, as a general rule, the concentrations of suspended sediment observed in the summer period are higher than the concentrations observed for an identical discharge in the winter period, even when the sample is taken during the rising phase of the flood in the studied stations. In addition, it was observed that this difference between the concentration of samples in winter and in summer is maximum in the small watersheds located in silty areas. Large-area watersheds are less subject to this phenomenon of temporal differentiation because the impact of runoff due to summer storms is integrated over the entire surface.

Despite the high variability of factors controlling the sediment yields (Zabaleta et al. 2016), the physical characteristics of the watersheds play a role in sediment yield. In addition to the scale effect of their area, it has been demonstrated that parameters such as slope, land cover, lithology, and soil erosivity have an effect on sediment budget (Van Oost et al. 2000; Yan et al. 2013; de Vente et al. 2013; Fang et al. 2016; Messina and Biggs 2016). Moreover, the link between higher drainage density and higher sediment yield is only present in homogeneous bedrock geology (Dragičević et al. 2018). In addition, the connectivity of the river networks also plays a significant role. The presence of weirs and dams impacts the

fine sediment transport (Lajczak, 1996). In urban area, the rectified reaches also affect its transport by the narrowing due to bridges and hydraulic obstacles. Even if the land cover data are not sufficient to realistically represent all the sedimentary processes that take place from soil erosion to the outlet and the accumulation processes, the more complex models are generally very difficult to calibrate for large watersheds. The use of Corine Land Cover maps with a resolution of 100 m was the only available technique to compare different years with thematic consistency over the last decades. Due to the international environment of the studied watersheds, pan-European data are needed to deal with the part of them that are in boundary countries and regions.

Compilation studies often highlight the influence of runoff in the variability of SSY. In Wallonia, Perpinien (1998) observed very low denudation rates at the level of the Mehaigne, at its confluence with the Meuse (14 t km^{-2} year^{-1} at Wanze in 1997), while Sine and Agneessens (1978) observed a SSY of barely 10 t km^{-2} year^{-1} in the upper Mehaigne (20.4 km^2). These differences highlight the great interannual variability of SSY which makes it difficult to compare the values based on different analysis periods, especially when they include particularly dry years, such as the 1973–1977 period studied by Sine and Agneessens (Lamalle et al. 1989). The results of Vanmaercke et al. (2012b) with a worldwide dataset remain inconclusive about the potential impact of land use on the inter-annual variability of SSY, but indicate a weak correlation. Costa et al. (2017) only managed to observe a link with land cover modifications over a 40-year period of data with continuous monitoring in an Alpine environment.

This study has demonstrated that nowadays the rivers that were suspected of clogging the downstream waterways, such as the Trouille River and the Samme River, did not represent a massive input of sediment each year. However, taking into account the estimated value by the public managers of 1.3 million tons of accumulated sediment in the Condé-Pommeroeul canal since 1818 (connected to the Trouille River via the Haine River) and the data from the station #40 (Trouille River at Hyon, with a watershed area of 224 km^2 and a median SSY of 28.4 t km^{-2} year^{-1}), the simple extrapolation by multiplication of our median SSY results over the period 1818–2010 reaches 1.22 million tons of potentially accumulated suspended sediment for this 192-year period. The computation by other means of the sediment yield was in accordance with the results found in our study. For instance and despite the difference in watershed area, the SSY was estimated to be between 28 and 33 t km^{-2} year^{-1} with an accumulation in the Bütgenbach dam from 1932 to 2004 (Hallot et al. 2012) compared to 30 t km^{-2} year^{-1} of median 1996–2018 SSY value with suspended sediment samplings.

Several types of potential uncertainty were addressed in the computation of the SSY from sediment rating curves. The first type is due to the sampling method and the representativeness of the sample across the water column and the water section. Perpinien (1998) observed, thanks to measurements conducted by Lamalle (1987) in the Burdinale River and Pironet (1995) in the Magne River, a low variability in suspended sediment concentration of samples taken at different depths on cross-sections. This variability is different with average concentrations. The coefficient of variation is 8 to 12% for average concentrations below 30 mg l^{-1}, between 1.3 and 6% for average concentrations of 150 to 600 mg l^{-1} and 8.4% for a concentration of 1800 mg l^{-1} on the Burdinale River. The second type of uncertainty relates to the quality of the sediment rating curve, linked to the trap efficiency of the filtration method and the ability for modelling suspended sediment concentration across a wide range of discharge. Jung et al. (2020) summarize a computing method of several validation criteria to describe the quality of the sediment rating curve. Another source of uncertainty in the SSY computation is the model of interpolation of annual or pluri-annual sediment yield. A great variety of types of calculations exist to interpolate from infrequent samples (Phillips et al. 1999; Delmas et al. 2011). The summation of modelled concentrations on an hourly discharge basis was used in this study. However, each type of computation model may give very different SSY results, in relation to the number of samples, the coefficient of determination of the sediment rating curve, and the distribution of the samples over the range of flow discharge values. Estimating sediment yield over large watersheds is a difficult task, taking into account the great spatial and temporal variability of physical parameters of the watersheds, and the difficulty of sampling with representativeness the suspended sediment at a wide range of discharge values.

The frequency of suspended sediment sampling also has a non-negligible impact on the annual sediment yield calculated from the flow series (Horowitz 2002, 2003; Vanmaercke et al. 2012b; Skarbøvik et al. 2012). Walling (1977) showed significant differences in the interpolation of SSY with different sampling timings such as daily, monthly or seasonal intervals. Underestimates of up to 70% are reported in the literature when the sampling frequency is weekly (Li et al. 2006). A fairly small number of samples, for example 12 samples taken on a hydrological basis rather than a calendar basis, may allow a first estimate of the annual sediment transport to be obtained while minimizing the trips required to cover a large network of stations (Skarbøvik et al. 2012). The representativeness of the sediment rating curves obtained is correct for the majority of the study sites. However, the number of samples or the range of sampled discharges was too small in 10 cases, leading to unsatisfactory results. This

compromise between the precision of the estimate of the annual sediment yield and the ability of sampling a large number of measurement sites is dependent upon each watershed, because the bias due to a low sampling frequency can vary greatly with the area and physical characteristics of the studied watersheds (Moatar et al. 2006).

In the end, the source data of land cover maps, their reference year, and their resolution may be another issue affecting the multicriteria analyses. With a variable sampling period for the studied sites, the land cover map at different epochs has been used and integrated to the searching for correlations between land cover and the SSY at the outlet of the watershed. The Corine Land Cover map for the year 2006 has shown better correlation values compared to ProbaV 2015 maps (Buchhorn et al. 2019), previously tested. The current trend of urbanizing the areas in the agricultural area such as the Hesbaye and the Brabant Plateau region could lead to an increase of the sediment transport by raising the connectivity of the sediment source and the rivers downstream through the impervious area.

5 Conclusions

Since the end of the 1990s, campaigns of suspended sediment samplings have been carried out on 72 study sites in the Southern part of Belgium in order to acquire sediment yields at the outlet of watersheds located in different geographical regions. The statistical validity and representativeness of the sediment curves has been described using several descriptors. This type of study aiming at accumulating many suspended sediment samples from a great number of gauging stations confronted us with the difficulty of obtaining representative results at different time and space scales. The classical method of interpolation of the suspended sediment concentration with the Ferguson correction required by the bi-logarithmic space was the methodology used to compute the SSY over a representative period with the available series of hourly discharges. However, the high variability of SSY related to the seasonality of sediment transport in fluvial regimes would, due to logistics and costs, tend to result in only a small number of stations, representative of geographic regions or watersheds, being equipped with continuous measurement devices to acquire data during single events. The methodology described here made it possible to obtain an order of magnitude of the sediment transport in suspension for a large number of stations, which was the initial request of the river managers.

Belonging to seven very different geographical regions, with their specific geologic substratum, type of soils, and land cover, differences in SSY have been observed. Considering the computed data for valid sediment rating curves,

median SSY reaches, on average, 20.1 t km^{-2} year^{-1} in Lorraine, 28.7 t km^{-2} year^{-1} in Ardenne, 52.9 t km^{-2} year^{-1} in the Haine basin, 30.7 t km^{-2} year^{-1} in Fagne-Famenne, 96.1 t km^{-2} year^{-1} in Hesbaye, 63.2 t km^{-2} year^{-1} in Entre-Vesdre-et-Meuse, and 192.2 t km^{-2} year^{-1} in the Brabant Plateau region. The estimated SSC value at bankfull discharge was related to the proportion of agricultural areas in the watershed ($R^2 = 0.60$). Indeed, rivers from Ardenne, Fagne, and Famenne regions and the northern part of the Lorraine region depict low SSC at Q_b. Conversely, Brabant Plateau and Hesbaye rivers (and to a lesser extent, those located in the southern part of Lorraine) show the larger sediment concentrations at bankfull discharge, correlated to a predominantly agricultural land cover. The percentage of cultivated areas (in 2006) is weakly correlated with median SSY of the 1996–2018 period ($R = 0.42$), while the percentage of forested areas ($R = -0.45$) is inversely correlated with sediment yields. The mean slope of the watershed ($R = -0.28$) and the average elevation ($R = -0.43$) present an inverse trend in comparison to the median SSY, but the mean elevation is linked to the proportion of agricultural areas in terms of climatic environment and the availability of arable lands in Wallonia.

Compared to other sediment transport analyses, the order of magnitude of median SSY (33 t km^{-2} year^{-1}) was consistent with other studies in the same climatic context and for the same range of watershed areas. This study also confirms the great temporal and spatial variability of SSY. In terms of clogging of the waterways and dams, the computations made from sediment rating curves and hydrological data matched with the estimates of accumulated sediment over different time intervals.

The uncertainties that are linked to the sampling methods, the quality of the sediment rating curves in terms of representativeness, and the soundness of the choice of the available computation methods still make complex today the study of sediment transport in rivers. Further analyses that are based upon high-frequency water samplings and long-term data gathering would be necessary to define more precisely the intrinsic and complex sedimentary processes that take place in watersheds.

References

Araujo HA, Cooper AB, Hassan MA, Venditti J (2012) Estimating suspended sediment concentrations in areas with limited hydrological data using a mixed-effects model. Hydrol Process 26:3678–3688. https://doi.org/10.1002/hyp.8462

Asselman NEM (2000) Fitting and interpretation of sediment rating curves. J Hydrol 234:228–248. https://doi.org/10.1016/S0022-1694(00)00253-5

Boardman J, Poesen J (2006) Soil erosion in Europe. John Wiley & Sons, Ltd

Buchhorn M, Smets B, Bertels L et al (2019) Copernicus Global Land Service: Land Cover 100 m: epoch 2015: Globe. Dataset of the global component of the Copernicus Land Monitoring Service

Campbell FB, Bauder HA (1940) A rating-curve method for determining silt-discharge of streams. Trans Am Geophys Union 21:603–607

Cerdan O, Delmas M, Négrel P et al (2012) Contribution of diffuse hillslope erosion to the sediment export of French rivers. C R Geosci 344:636–645. https://doi.org/10.1016/j.crte.2012.10.011

Close-Lecocq J-F, Pissart A, Koch G (1982) Les transports en suspension et en solution de la Meuse à Liège et à Tailfer (amont de Namur). Bull La Société Géographique Liège 18:5–18

Cohn TA, Delong LL, Gilroy EJ et al (1989) Estimating constituent loads. Water Resour Res 25:937–942. https://doi.org/10.1029/WR025i005p00937

Collins AL, Naden PS, Sear DA et al (2011) Sediment targets for informing river catchment management: international experience and prospects. Hydrol Process 25:2112–2129. https://doi.org/10.1002/hyp.7965

CORINE Land Cover (2018) CORINE Land Cover raster data (CLC1990, CLC2000, CLC2006, CLC2012 and CLC2018) — European Environment Agency

Costa A, Anghileri D, Molnar P (2017) A Process–based rating curve to model suspended sediment concentration in Alpine environments Hydrol Earth Syst Sci Discuss 1–23. https://doi.org/10.5194/hess-2017-419

Davis WM (1899) The Geographical Cycle. Geogr J 14:481. https://doi.org/10.2307/1774538

de Béthune P (1954) Géologie de la Belgique, carte à l'échelle 1/500.000. Atlas de Belgique, planche 8

de Vente J, Poesen J, Bazzoffi P et al (2006) Predicting catchment sediment yield in Mediterranean environments: the importance of sediment sources and connectivity in Italian drainage basins. Earth Surf Proc Land 31:1017–1034. https://doi.org/10.1002/esp.1305

de Vente J, Poesen J, Verstraeten G et al (2013) Predicting soil erosion and sediment yield at regional scales: Where do we stand? Earth-Science Rev 127:16–29. https://doi.org/10.1016/j.earscirev.2013.08.014

Dejonghe L (2007) Guide de lecture des cartes géologiques de Wallonie, 3e édition. Ministère de la Région wallonne, Direction des Ressources naturelles et de l'Environnement

Delmas M, Cerdan O, Cheviron B, Mouchel JM (2011) River basin sediment flux assessments. Hydrol Process 25:1587–1596. https://doi.org/10.1002/hyp.7920

Demoulin A (2012) Morphometric dating of the fluvial landscape response to a tectonic perturbation. Geophys Res Lett 39:1–5. https://doi.org/10.1029/2012GL052201

Denis A-C, Van Campenhout J, Bouffioux A et al (2014) Quantitative and qualitative evaluation of sediment and contaminant transport in the Samme river catchment (Brabant region - Belgium). In: Maggioli Editore (ed) Proceedings of 4th International Symposium on Sediment Management. Ferrara, Italy, pp 475–482

Deroanne C (1995) Dynamique fluviale de la Hoëgne. Évaluation longitudinale des caractéristiques sédimentologiques du lit et des paramètres de mobilisation de la charge de fond. Mémoire de licence en Sciences géographiques, Département de Géographie. Université de Liège

Doomen AMC, Wijma E, Zwolsman JJG, Middelkoop H (2008) Predicting suspended sediment concentrations in the Meuse river using a supply-based rating curve. Hydrol Process 22:1846–1856. https://doi.org/10.1002/hyp.6767

Dragičević N, Karleuša B, Ožanić N (2018) Improvement of drainage density parameter estimation within erosion potential method. Proceedings 2:620. https://doi.org/10.3390/proceedings2110620

Dumas D (2007) The results of 10 years of daily observations of the flux of suspended matter in one of the main watercourses in the European Alps: the Isere at Grenoble (France). C R Geosci 339:810–819. https://doi.org/10.1016/j.crte.2007.09.003

Erpicum M, Nouri M, Demoulin A (2018) The climate of Belgium and Luxembourg. In: Demoulin A (ed) Landscapes and landforms of Belgium and Luxembourg. Springer International Publishing, Cham, pp 35–41

Estrany J, Garcia C, Batalla RJ (2009) Suspended sediment transport in a small Mediterranean agricultural catchment. Earth Surf Proc Land 34:929–940. https://doi.org/10.1002/esp.1777

Evrard O, Bielders CL, Vandaele K, van Wesemael B (2007) Spatial and temporal variation of muddy floods in central Belgium, off-site impacts and potential control measures. CATENA 70:443–454. https://doi.org/10.1016/j.catena.2006.11.011

Fang NF, Chen FX, Zhang HY et al (2016) Effects of cultivation and reforestation on suspended sediment concentrations: A case study in a mountainous catchment in China. Hydrol Earth Syst Sci 20:13–25. https://doi.org/10.5194/hess-20-13-2016

Ferguson RI (1986) River loads underestimated by rating curves. Water Resour Res 22:74–76

Ferguson RI (1987) Accuracy and precision of methods for estimating river loads. Earth Surf Proc Land 12:95–104. https://doi.org/10.1002/esp.3290120111

Fortesa J, Ricci GF, García-Comendador J et al (2021) Analysing hydrological and sediment transport regime in two Mediterranean intermittent rivers. CATENA 196:104865. https://doi.org/10.1016/j.catena.2020.104865

Franchimont C (1993) Dynamique fluviale de la Lesse : fréquence des inondations, morphométrie des méandres et sédimentologie du lit. Mémoire de licence en Sciences géographiques, Département de Géographie. Université de Liège

Furuichi T, Win Z, Wasson RJ (2009) Discharge and suspended sediment transport in the Ayeyarwady River, Myanmar: centennial and decadal changes. Hydrol Process 23:1631–1641. https://doi.org/10.1002/hyp.7295

Gao P, Josefson M (2012) Temporal variations of suspended sediment transport in Oneida Creek watershed, central New York. J Hydrol 426–427:17–27. https://doi.org/10.1016/j.jhydrol.2012.01.012

Gericke A, Venohr M (2012) Improving the estimation of erosion-related suspended solid yields in mountainous, non-alpine river catchments. Environ Model Softw 37:30–40. https://doi.org/10.1016/j.envsoft.2012.04.008

Grasso DA, Jakob A (2003) Charge de sédiments en suspension : comparaison entre deux méthodes de calcul. GWA 83:898–905

Grauso S, Fattoruso G, Crocetti C, Montanari A (2008) Estimating the suspended sediment yield in a river network by means of geomorphic parameters and regression relationships. Hydrol Earth Syst Sci 12:177–191. https://doi.org/10.5194/hess-12-177-2008

Gravelius H (1914) Grundriß der gesamten Gewcisserkunde. Band I: Flußkunde (Compendium of Hydrology, Vol. I. Rivers, in German). Goschen, Berlin

Hallot E (2010) Typologie hydro-géomorphologique des cours d'eau dans l'Euregio Meuse-Rhin. Thèse de doctorat, Département de Géographie. Université de Liège.

Hallot E, Benoit M, Stasse G et al (2012) L'envasement du lac de Butgenbach (Ardenne, Belgique). Bull La Société Géographique Liège 59:39–57

Hart EA, Schurger SG (2005) Sediment storage and yield in an urbanized karst watershed. Geomorphology 70:85–96. https://doi.org/10.1016/j.geomorph.2005.04.002

Higgins A, Restrepo JC, Ortiz JC et al (2013) Suspended sediment transport in the Magdalena River (Colombia, South America): Hydrologic regime, rating parameters and effective discharge variability. Int J Sediment Res 31:25–35. https://doi.org/10.1016/j.ijsrc.2015.04.003

Hombrouckx N (2002) Analyse hydrologique du bassin de la Gette. Identification et récurrence du débit à pleins bords. Zones inondables et localisation de l'habitat. Transports en solution et en suspension. Mémoire de licence en Sciences géographiques, Département de Géographie. Université de Liège

Horowitz AJ (2002) The use of rating (transport) curves to predict suspended sediment. In: Turbidity and other sediment surrogates workshop, April 30. Reno, Nevada

Horowitz AJ (2003) An evaluation of sediment rating curves for estimating suspended sediment concentrations for subsequent flux calculations. Hydrol Process 17:3387–3409. https://doi.org/10.1002/hyp.1299

Houbrechts G (2000) Utilisation des macroscories comme indicateur du transport de la charge de fond des rivières de la «Terre de Durbuy». Mémoire de licence en Sciences géographiques, Département de Géographie. Université de Liège.

Houbrechts G (2005) Utilisation des macroscories et des microscories en dynamique fluviale : application aux rivières du massif ardennais (Belgique). Thèse de doctorat, Département de Géographie. Université de Liège.

Houbrechts G, Levecq Y, Peeters A et al (2015) Evaluation of long-term bedload virtual velocity in gravel-bed rivers (Ardenne, Belgium). Geomorphology 251:6–19. https://doi.org/10.1016/j.geomorph.2015.05.012

Jansson M (1985) A comparison of detransformed logarithmic regressions and power function regressions. Geogr Ann Ser A, Phys Geogr 67:61. https://doi.org/10.2307/520466

Jansson MB (1996) Estimating a sediment rating curve of the Reventazon river at Palomo using logged mean loads within discharge classes. J Hydrol 183:227–241

Jung BM, Fernandes EH, Möller OOM, García-Rodríguez F (2020) Estimating suspended sediment concentrations from river discharge data for reconstructing gaps of information of long-term variability studies. Water 12:2382. https://doi.org/10.3390/w12092382

Keaton JR (2019) Review of contemporary terminology for damaging surficial processes – Stream flow, hyperconcentrated sediment flow, debris flow, mud flow, mud flood, mudslide. Debris-Flow Hazards Mitig Mech Monit Model Assess - Proc 7th Int Conf Debris-Flow Hazards Mitig 748–757

Koch RW, Smillie GM (1986) Bias in hydrologic prediction using log-transformed regression models. J Am Water Resour Assoc 22:717–723

Lajczak A (1996) Modelling the long-term course of non-flushed reservoir sedimentation and estimating the life of dams. Earth Surf Proc Land 21:1091–1107. https://doi.org/10.1002/(SICI)1096-9837(199612)21:12%3C1091::AID-ESP653%3E3.0.CO;2-2

Lamalle C (1987) Les transports en suspension et en solution dans la Burdinale. Mémoire de licence en Sciences géographiques, Département de Géographie. Université de Liège

Lamalle C, Petit F, Koch G et al (1989) Les transports en suspension et en solution dans la Burdinale, affluent principal de la Mehaigne. Bull La Société Géographique Liège 25:39–51

Lane PNJ, Sheridan GJ, Noske PJ (2006) Changes in sediment loads and discharge from small mountain catchments following wildfire in south eastern Australia. J Hydrol 331:495–510. https://doi.org/10.1016/j.jhydrol.2006.05.035

Lefrançois J, Grimaldi C, Gascuel-Odoux C, Gilliet N (2007) Suspended sediment and discharge relationships to identify bank degradation as a main sediment source on small agricultural catchments. Hydrol Process 21:2923–2933. https://doi.org/10.1002/hyp.6509

Lemin G (1984) Contribution à l'étude des transports solides dans des rivières du bassin de la Meuse (Meuse, Ourthe, Hoëgne). Mémoire de licence en Sciences géographiques, Département de Géographie. Université de Liège.

Lemin G, Koch G, Hurtgen C, Pissart A (1987) Les transports en suspension de la Meuse, l'Ourthe et la Hoëgne. Bull La Société Géographique Liège 22–23:39–61

Lenzi MA, Marchi L (2000) Suspended sediment load during floods in a small stream of the Dolomites (northeastern Italy). CATENA 39:267–282. https://doi.org/10.1016/S0341-8162(00)00079-5

Li F-C, Angelier J, Chen R-F et al (2005) Estimates of present-day erosion based on sediment transport in rivers: a case study in Taiwan. C R Geosci 337:1131–1139. https://doi.org/10.1016/j.crte.2005.05.001

Li Z, Zhang Y-K, Schilling K, Skopec M (2006) Cokriging estimation of daily suspended sediment loads. J Hydrol 327:389–398. https://doi.org/10.1016/j.jhydrol.2005.11.028

Louette F (1995) Évaluation du débit à pleins bords et de sa récurrence dans plusieurs rivières de Moyenne et Haute Belgique. Mémoire de licence en Sciences géographiques, Département de Géographie. Université de Liège.

Mabille G, Petit F (1987) Influence des aménagements du cours d'une rivière de Moyenne Belgique et de son bassin hydrographique, sur le comportement hydrologique de la rivière. In: Crues et inondations. Humbert J. et al., Strasbourg, pp 279–293

Mano V, Nemery J, Belleudy P, Poirel A (2009) Assessment of suspended sediment transport in four alpine watersheds (France): influence of the climatic regime. Hydrol Process 23:777–792. https://doi.org/10.1002/hyp.7178

Marttila H, Kløve B (2010) Dynamics of erosion and suspended sediment transport from drained peatland forestry. J Hydrol 388:414–425. https://doi.org/10.1016/j.jhydrol.2010.05.026

McKerchar AI (2003) Streamflow. In: Meyers (Ed), Encyclopedia of physical science and technology (Third Edition). Academic Press, New York, pp 129–142. doi:https://doi.org/10.1016/B0-12-227410-5/00741-9

Messina AM, Biggs TW (2016) Contributions of human activities to suspended sediment yield during storm events from a small, steep, tropical watershed. J Hydrol 538:726–742. https://doi.org/10.1016/j.jhydrol.2016.03.053

Métadier M, Bertrand-Krajewski J-L (2012) The use of long-term on-line turbidity measurements for the calculation of urban stormwater pollutant concentrations, loads, pollutographs and intra-event fluxes. Water Res 46:6836–6856

Meybeck M, Laroche L, Dürr HH, Syvitski JPM (2003) Global variability of daily total suspended solids and their fluxes in rivers. Glob Planet Change 39:65–93. https://doi.org/10.1016/S0921-8181(03)00018-3

Moatar F, Person G, Meybeck M et al (2006) The influence of contrasting suspended particulate matter transport regimes on the bias and precision of flux estimates. Sci Total Environ 370:515–531. https://doi.org/10.1016/j.scitotenv.2006.07.029

Mols J (2004) Dynamique fluviale en réponse aux changements d'affectation du sol des bassins versants de l'Euregio Meuse-Rhin. Mémoire de DEA en Sciences, Département de Géographie. Université de Liège.

Monseur P (2005) Contribution à l'analyse du transport en suspension de rivières de Moyenne et de Haute Belgique. Application et étude spécifique d'une rivière de l'Entre Vesdre et Meuse (la Gulpe). Mémoire de licence en Sciences géographiques, Département de Géographie. Université de Liège.

Moriasi DN, Arnold JG, Van Liew MW et al (2007) Model evaluation guidelines for systematic quantification of accuracy in watershed simulations. Trans ASABE 50:885–900. https://doi.org/10.13031/2013.23153

Nadal-Romero E, Regüés D, Latron J (2008) Relationships among rainfall, runoff, and suspended sediment in a small catchment with badlands. CATENA 74:127–136. https://doi.org/10.1016/j.catena.2008.03.014

Navratil O, Esteves M, Legout C et al (2011) Global uncertainty analysis of suspended sediment monitoring using turbidimeter in a small mountainous river catchment. J Hydrol 398:246–259. https://doi.org/10.1016/j.jhydrol.2010.12.025

Ndomba P, Mtalo F, Killingtveit Å (2008) Developing an excellent sediment rating curve from one hydrological year sampling programme data: approach. J Urban Environ Eng 2:21–27. https://doi.org/10.4090/juee.2008.v2n1.021027

Oeurng C, Sauvage S, Sánchez-Pérez J-M (2010) Dynamics of suspended sediment transport and yield in a large agricultural catchment, southwest France. Earth Surf Proc Land 35:1289–1301. https://doi.org/10.1002/esp.1971

Panagos P, Borrelli P, Meusburger K et al (2015) Estimating the soil erosion cover-management factor at the European scale. Land Use Policy 48:38–50. https://doi.org/10.1016/j.landusepol.2015.05.021

Parkinson D, Petit F, Perpinien G, Philippart J-C (1999) Habitats de reproduction des poissons et processus géomorphologiques dans des rivières à fond caillouteux. Essai de synthèse et applications à quelques rivières du bassin de la Meuse. Bull La Société Géographique Liège 36:31–52

Pauquet A, Petit F (1993) Evolution de la fréquence des inondations de l'Ourthe inférieure. Bull La Société Belge d'Etudes Géographiques 2:361–375

Peeters A, Houbrechts G, de le Court B, et al (2021) Suitability and sustainability of spawning gravel placement in degraded river reaches. Belgium Catena 201:105217. https://doi.org/10.1016/j.catena.2021.105217

Peeters A, Houbrechts G, Hallot E et al (2018) Efficacité et résistance de techniques de protection de berges en génie végétal Géomorphologie Reli Process Environ 24. https://doi.org/10.4000/geomorphologie.11927

Peeters A, Houbrechts G, Hallot E et al (2020) Can coarse bedload pass through weirs? Geomorphology 359:107131. https://doi.org/10.1016/j.geomorph.2020.107131

Perpinien G (1998) Dynamique fluviale de la Mehaigne. Morphométrie, transports en solution et en suspension, mobilisation de la charge de fond. Mémoire de licence en Sciences géographiques, Département de Géographie. Université de Liège

Petit F (1983) Les processus de façonnement en milieu naturel du lit d'une rivière à sédiment limono-caillouteux. La Rulles en forêt d'Anlier. Thèse de doctorat en Sciences géographiques, Département de Géographie. Université de Liège

Petit F (1985) L'évolution de la charge en suspension d'une rivière ardennaise au cours de ses périodes de crues. Bull La Société Géographique Liège 21:97–104

Petit F (1987) The relationship between shear stress and the shaping of the bed of a pebble-loaded river, La Rulles - Ardenne.

CATENA 14:453–468. https://doi.org/10.1016/0341-8162(87)90015-4

Petit F, Daxhelet C (1989) Détermination du débit à pleins bords et de sa récurrence dans différentes rivières de moyenne et haute Belgique. Bull La Société Géographique Liège 25:69–84

Petit F, Hallot E, Houbrechts G et al (2007) La typologie et les caractéristiques hydromorphologiques des cours d'eau wallons. In: La gestion physique des cours d'eau: bilan d'une décennie d'ingénierie écologique. Direction des Cours d'Eau Non Navigables, Direction Générale des Ressources Naturelles et de l'Environnement - Ministère de la Région wallonne, Namur, pp 7–16

Petit F, Houbrechts G, Peeters A et al (2015) Dimensionless critical shear stress in gravel-bed rivers. Geomorphology 250:308–320. https://doi.org/10.1016/j.geomorph.2015.09.008

Petit F, Pauquet A (1997) Bankfull discharge recurrence interval in gravel-bed rivers. Earth Surf Proc Land 22:685–693. https://doi.org/10.1002/(SICI)1096-9837(199707)22:7%3c685::AID-ESP744%3e3.0.CO;2-J

Phillips JM, Webb BW, Walling DE, Leeks GJL (1999) Estimating the suspended sediment loads of rivers in the LOIS study area using infrequent samples. Hydrol Process 13:1035–1050

Picouet C, Hingray B, Olivry J-C (2009) Modelling the suspended sediment dynamics of a large tropical river: the Upper Niger River basin at Banankoro. Hydrol Process 23:3193–3200. https://doi.org/10.1002/hyp.7398

Pineux N (2018) Redistribution du sol au sein d'un bassin versant agricole : méthodes de mesure novatrices et essai de modélisation. Thèse de doctorat en Sciences agronomiques et ingénierie biologique. Gembloux Agro-Bio Tech - Université de Liège.

Pironet C (1995) Régime hydrologique, transports de sédiments et dynamique fluviale de la Magne. Rivière de sud-ouest du Plateau de Herve. Mémoire de licence en Sciences géographiques, Département de Géographie. Université de Liège

Ritchie JC (2007) Soil erosion and sediment redistribution in river catchments. Soil Sci 172(11):941. https://doi.org/10.1097/ss.0b013e318158a028

Roche M (1963) Hydrologie de surface. Gauthier-Villars ORSTOM, Paris

Rodríguez-Blanco ML, Taboada-Castro MM, Palleiro L, Taboada-Castro MT (2010) Temporal changes in suspended sediment transport in an Atlantic catchment, NW Spain. Geomorphology 123:181–188. https://doi.org/10.1016/j.geomorph.2010.07.015

Rovira A, Batalla RJ (2006) Temporal distribution of suspended sediment transport in a Mediterranean basin: The Lower Tordera (NE Spain). Geomorphology 79:58–71. https://doi.org/10.1016/j.geomorph.2005.09.016

Sadeghi SHR, Mizuyama T, Miyata S et al (2008) Development, evaluation and interpretation of sediment rating curves for a Japanese small mountainous reforested watershed. Geoderma 144:198–211. https://doi.org/10.1016/j.geoderma.2007.11.008

Seeger M, Errea M-P, Beguería S, et al (2004) Catchment soil moisture and rainfall characteristics as determinant factors for discharge/suspended sediment hysteretic loops in a small headwater catchment in the Spanish pyrenees. J Hydrol 288:299–311. https://doi.org/10.1016/j.jhydrol.2003.10.012

Sine L, Agneessens J-P (1978) Etude des débits solides et du phénomène de migration dans une rivière drainant un bassin agricole. Pédologie XXVIII:183–191

Skarbøvik E, Stålnacke P, Bogen J, Bønsnes TE (2012) Impact of sampling frequency on mean concentrations and estimated loads of suspended sediment in a Norwegian river: implications for water management. Sci Total Environ 433:462–471. https://doi.org/10.1016/j.scitotenv.2012.06.072

Smith HG (2007) Estimation of suspended sediment loads and delivery in an incised upland headwater catchment, south-eastern

Australia. Hydrol Process 22:3135–3148. https://doi.org/10.1002/hyp.6898

Spring W, Prost E (1884) Etude sur les eaux de la Meuse : Détermination des quantités de matières diverses roulées par les eaux de ce fleuve pendant l'espace d'une année. Ann la Société géologique Belgique XI:1651–1693

Steegen A, Govers G, Beuselinck L et al (1998) Variations in sediment yield from an agricultural drainage basin in central Belgium. IAHS Publ 177–185

Strahler AN (1952) Hypsometric (area-altitude) analysis of erosional topography. Geol Soc Am Bull 63:1117–1142. https://doi.org/10.1130/0016-7606(1952)63

Syvitski JP, Morehead MD, Bahr DB, Mulder T (2000) Estimating fluvial sediment transport : The rating parameters parameters (a and b) are defined by a power law relating discharge values of a river mathematical concentration is inversely proportional to the long-term. Water Resour Res 36:2747–2760. https://doi.org/10.1029/2000WR900133

Tena A, Batalla RJ, Vericat D, López-Tarazón JA (2011) Suspended sediment dynamics in a large regulated river over a 10-year period (the lower Ebro, NE Iberian Peninsula). Geomorphology 125:73–84. https://doi.org/10.1016/j.geomorph.2010.07.029

Thomas RB (1985) Estimating total suspended sediment yield with probability sampling. Water Resour Res 21:1381–1388. https://doi.org/10.1029/WR021i009p01381

Tramblay Y, Saint-Hilaire A, Ouarda TBMJ et al (2010) Estimation of local extreme suspended sediment concentrations in California Rivers. Sci Total Environ 408:4221–4229. https://doi.org/10.1016/j.scitotenv.2010.05.001

Vaessen Q, Houbrechts G, Peeters A, Van Campenhout J (2021) Caractéristiques hydro-géomorphologiques des microhabitats d'Unio crassus (Ardenne, Belgique). Géomorphologie Reli Process Environ 27:3–18. https://doi.org/10.4000/geomorphologie.15113

Van Campenhout J, Denis A-C, Hallot E et al (2013) Flux des sédiments en suspension dans les rivières du bassin de la Meuse : proposition d'une typologie régionale basée sur la dénudation spécifique des bassins versants. Bull La Société Géographique Liège 61:15–36

Van Campenhout J, Hallot E, Houbrechts G et al (2015) Flash floods and muddy floods in Wallonia: recent temporal trends, spatial distribution and reconstruction of the hydrosedimentological fluxes using flood marks and sediment deposits. Belgeo 1:1–22

Van Campenhout J, Houbrechts G, Peeters A, Petit F (2020) Return period of characteristic discharges from the comparison between partial duration and annual series. Application to the Walloon Rivers Water (switzerland) 12:792. https://doi.org/10.3390/w12030792

Van Oost K, Govers G, Desmet P (2000) Evaluating the effects of changes in landscape structure on soil erosion by water and tillage. Landsc Ecol 15:577–589. https://doi.org/10.1023/A:1008198215674

Vanmaercke M, Maetens W, Poesen J et al (2012a) A comparison of measured catchment sediment yields with measured and predicted hillslope erosion rates in Europe. J Soils Sediments 12:586–602. https://doi.org/10.1007/s11368-012-0479-z

Vanmaercke M, Poesen J, Govers G, Verstraeten G (2015) Quantifying human impacts on catchment sediment yield: a continental approach. Glob Planet Change 130:22–36. https://doi.org/10.1016/j.gloplacha.2015.04.001

Vanmaercke M, Poesen J, Radoane M et al (2012b) How long should we measure? An exploration of factors controlling the interannual variation of catchment sediment yield. J Soils Sediments 12:603–619. https://doi.org/10.1007/s11368-012-0475-3

Vanmaercke M, Poesen J, Verstraeten G et al (2011) Sediment yield in Europe: spatial patterns and scale dependency. Geomorphology 130:142–161. https://doi.org/10.1016/j.geomorph.2011.03.010

Verstraeten G, Poesen J (2001) Factors controlling sediment yield from small intensively cultivated catchments in a temperate humid climate. Geomorphology 40:123–144. https://doi.org/10.1016/S0169-555X(01)00040-X

Verstraeten G, Poesen J, de Vente J, Koninckx X (2003) Sediment yield variability in Spain: A quantitative and semiqualitative analysis using reservoir sedimentation rates. Geomorphology 50:327–348. https://doi.org/10.1016/S0169-555X(02)00220-9

Walling DE (1977) Limitations of the rating curve technique for estimating suspended sediment loads, with particular reference to British rivers. In: Erosion and Solid Matter Transport in Inland Waters (Proc. Paris Symp., July 1977). IAHS Publ 122:34–48

Ward PJ (2008) River Meuse suspended sediment yield: a new estimate and past estimates revisited. Geo Impuls 87:189–193

Warrick JA (2015) Trend analyses with river sediment rating curves. Hydrol Process 29:936–949. https://doi.org/10.1002/hyp.10198

Warrick JA, Melack JM, Goodridge BM (2015) Sediment yields from small, steep coastal watersheds of California. J Hydrol Reg Stud 4:516–534. https://doi.org/10.1016/j.ejrh.2015.08.004

Webb BW, Phillips JM, Walling DE et al (1997) Load estimation methodologies for British rivers and their relevance to the LOIS RACS(R) programme. Sci Total Environ 194–195:379–389. https://doi.org/10.1016/S0048-9697(96)05377-6

Wilson BG, Adams BJ, Karney BW (1990) Bias in log-transformed frequency distributions. J Hydrol 118:19–37

Yan B, Fang NF, Zhang PC, Shi ZH (2013) Impacts of land use change on watershed streamflow and sediment yield: an assessment using hydrologic modelling and partial least squares regression. J Hydrol 484:26–37. https://doi.org/10.1016/j.jhydrol.2013.01.008

Zabaleta A, Antiguedad I, Barrio I, Probst JL (2016) Suspended sediment delivery from small catchments to the Bay of Biscay. What are the controlling factors? Earth Surf Proc Land 41:1894–1910. https://doi.org/10.1002/esp.3957

Zimmermann A, Francke T, Elsenbeer H (2012) Forests and erosion: Insights from a study of suspended-sediment dynamics in an overland flow-prone rainforest catchment. J Hydrol 428–429:170–181. https://doi.org/10.1016/j.jhydrol.2012.01.039